REGULATION OF RETINAL ACTIVITY IN AN *EX-VIVO* GUINEA PIG MODEL BY EFFECTS OF KETAMINE AND XYLAZINE ANESTHETICS

by

T. Jeffrey Locke

Submitted in partial fulfillment of the requirements
for the degree of Master of Science

at

Dalhousie University
Halifax, Nova Scotia
November 2018

Dedication Page

To my friends, family and colleagues who continuously encouraged me to succeed in this project even when I had doubts in myself.

Table of Contents

LIST OF TABLES v

LIST OF FIGURES vi

ABSTRACT ix

LIST OF ABBREVIATIONS AND SYMBOLS USED x

ACKNOWLEDGEMENTS xi

CHAPTER 1: INTRODUCTION 1

CHAPTER 2: ANESTHESIA 3

2.1 REVIEW OF DIFFERENT MECHANISMS OF ANESTHETICS 4

2.2 MOLECULAR ACTION 6

2.3 KETAMINE 8

2.4 XYLAZINE 11

CHAPTER 3: THE RETINA AS A MODEL 13

3.1 RETINAL ORGANIZATION 13

3.2 RETINAL PHYSIOLOGY/CIRCUITS 15

3.3 RETINAL GANGLION CELLS AS PROBE OF RETINAL OUTPUT 18

3.3.1 MULTIELECTRODE ARRAY TECHNOLOGY 22

CHAPTER 4: GUINEA PIG AS AN ANIMAL MODEL 25

CHAPTER 5: METHODS 28

5.1 PROTOCOLS 28

5.2 ANIMAL PREPERATION 28

5.3 PERFUSION SYSTEM 29

5.4 MEA RECORDING 31

5.5 SPIKE SORTING/FILTERING 33

5.6 PSTH DESCRIPTION 34

5.7 CELL CLASSIFICATION 34

5.8 COMPILATION OF RATIO 35

5.9 STATISTICAL ANALYSIS 36
CHAPTER 6: RESULTS 37
6.1.0 KETAMINE 37
6.1.1 GLOBAL EFFECT ON SPIKING RATIO 37
6.1.2 GLOBAL EFFECT ON CELL TYPE 43
6.2.0 XYLAZINE 50
6.2.1 GLOBAL EFFECT ON SPIKING RATIO 50
6.2.2 GLOBAL EFFECT ON CELL TYPE 57
6.3.0 COMBINED CONCENTRATION OF KETAMINE/XYLAZINE 64
6.3.1 GLOBAL EFFECT ON SPIKING RATIO 64
CHAPTER 7: DISCUSSION 71
7.1 IMPORTANT FINDINGS 71
7.2 TECHNICAL CONSIDERATIONS 73
7.3 PLASMA CONCENTRATIONS 73
7.4 EFFECT OF ANESTHETIC AGENTS ON NEURONAL FUNCTION 76
7.5 PROPOSED MECHANISM OF ACTION 78
7.6 LIMITATIONS 80
7.7 FUTURE STUDIES 82
7.8 CONCLUSION 83
REFERENCES 84

List of Tables

Table 1	Blood plasma levels sampled of ketamine and xylazine, after drug administration at various anesthetic and sub-anesthetic dosages in human and animal models.	31
Table 2	Measures of central tendency and variation for overall ketamine experiments at each concentration.	40
Table 3	Percent change in cell behavior in function of parts of the responses and cell types.	45
Table 4	Measures of central tendency and variation for overall xylazine experiments at each concentration.	54
Table 5	Percent change in cell behavior in function of parts of the responses and cell types.	58
Table 6	Measures of central tendency and variation for overall Ketamine + Xylazine experiments at each concentration.	67
Table 7	Known blood plasma concentrations at sub-anesthetic and clinical anesthetic concentrations with experimental drug concentrations used for MEA experimentation.	74

List of Figures

Figure 1	Schematic of the layers of the mammalian retina	15
Figure 2	Phototransduction cascade of a rod photoreceptor in response to a light stimulus.	19
Figure 3	Schematic representation of antagonistic center-surround receptive field organization.	20
Figure 4	Joint interspike interval (ISI) plot for the spike train of an ON_OFF DS cell in response to spatial white noise.	22
Figure 5	Multi-electrode Array System	24
Figure 6	Schematic of the MEA set-up	33
Figure 7	Retinal ganglion cell firing patterns.	35
Figure 8.1	Peristimulus time histogram of average RGC spiking activity (frequency) over time (ms) at multiple concentrations of ketamine. Normalized	38
Figure 8.2	Peristimulus time histogram of average RGC spiking activity (frequency) over time (ms) at multiple concentrations of ketamine.	39
Figure 9	Mean ratio of ganglion cell spiking activity (total response) in ketamine concentrations compared to baseline spiking activity for all cell spiking types, low activity, intermediate activity and high activity cells. Whole data shown for illustration, log transformed data used for statistical analysis.	42
Figure 10	Ratio of ganglion cell spiking of spontaneous activity, ON response and OFF response in ketamine concentrations compared to baseline spiking for all cells, low activity, intermediate activity and high activity cells	46
Figure 11	Estimated marginal means for the ratio of cell spiking at different ketamine concentrations for the overall experiment and for spontaneous cell spiking, ON cell spiking and OFF cell spiking.	49
Figure 12	Ratio of early response (first 300ms) to later response (last 400ms) for ON (Green) and OFF (Orange)	50

responses. Index of briskness of a response: S=Sluggish; P=Prompt. Ctl=baseline spontaneous activity; k=ketamine concentration (mg/ml).

Figure 13.1 Peristimulus time histogram of average RGC spiking activity (frequency) over time (ms) at multiple concentrations of xylazine. Normalized 52

Figure 13.2 Peristimulus time histogram of average RGC spiking activity (frequency) over time (ms) at multiple concentrations of xylazine. 53

Figure 14 Mean ratio of ganglion cell spiking activity (total response) in xylazine concentrations compared to baseline spiking activity for all cell spiking types, low activity, intermediate activity and high activity cells. 55

Figure 15 Ratio of ganglion cell spiking of spontaneous activity, ON response and OFF response in xylazine concentrations compared to baseline spiking for all cells, low activity, intermediate activity and high activity cells. 60

Figure 16 Estimated marginal means for the ratio of cell spiking at different xylazine concentrations for the overall experiment and for spontaneous cell spiking, ON cell spiking and OFF cell spiking. 63

Figure 17 Ratio of early response (first 300ms) to later response (last 400ms) for ON (Green) and OFF (Orange) responses. Index of briskness of a response: S=Sluggish; P=Prompt. Ctl=baseline spontaneous activity; X=xylazine concentration (mg/ml). 64

Figure 18.1 Peristimulus time histogram of average RGC spiking activity (normalized) over time (ms) at at ketamine 0.1mg/ml and ketamine 0.1mg/ml + xylazine 0.004mg/ml. xylazine 0.004mg/ml, from xylazine experiments, (right) for comparison. 65

Figure 18.2 Peristimulus time histogram of average RGC spiking activity (frequency) over time (ms) at ketamine 0.1mg/ml and ketamine 0.1mg/ml + xylazine 0.004mg/ml. xylazine 0.004mg/ml, from xylazine experiments, (right) for comparison. 66

Figure 19	Estimated marginal means for the ratio of cell spiking at ketamine 0.1 mg/ml and ketamine 0.1 mg/ml + xylazine 0.004 mg/ml concentrations for the overall experiment and for spontaneous cell spiking, ON cell spiking and OFF cell spiking.	69
Figure 20	Ratio of ganglion cell spiking activity (frequency) in Ketamine 0.1mg/ml (blue) and ketamine 0.1mg/ml + xylazine 0.004mg/ml (red) concentrations compared to baseline spiking activity for all cell spiking types, low activity, intermediate activity and high activity cells.	70
Figure 21	Ratio of ganglion cell spiking (frequency) in ketamine 0.01 mg/ml and ketamine 0.01mg/ml + xylazine 0.004mg/ml concentrations compared to baseline spiking for all cells, low activity, intermediate activity and high activity cells	70

Abstract

Anesthetic agents are commonly used for their desired effects during procedures and experiments in humans and animal models. Additional effects on neuronal function and behavior are still widely unknown. This report investigated the effects of various concentrations of two commonly used veterinary anesthetics, ketamine and xylazine, on the retinal ganglion cell spiking activity of an ex-vivo guinea pig retina. There was a main effect of ketamine concentration on the mean ganglion cell spiking, with lower concentrations increasing the ratio of cell spiking and the highest concentration showing a decline in the ratio. This observed effect appears to influence RGCs differently based on their tonicity. Similarly, with xylazine we observed a main effect of concentration with an increased ratio at lower concentrations and a decline at the highest concentration. When drugs were co-administered there was an effect based on the cell's tonicity.

List of Abbreviations and Symbols Used

AMPD	α-amino-3-hydroxy-5-methyl-4-isoxazolepropionic acid
Ca2+	calcium ion/ channel
CNS	central nervous system
ERG	electroretinogram
GABA	gamma-Aminobutyric acid
ISI	interspike interval
K+	potassium ion/ channel
Ket	ketamine
Mg2+	magnesium ion/ channel
MEA	multi-electrode array
Na+	sodium ion/ channel
NMDA	N-methy-D-aspartate
NREM	non-rapid eye movement sleep
PSTH	peristimulus time histogram
RGC	retinal ganglion cell
Xyl	xylazine
[]	concentration

Acknowledgements

I'd like to acknowledge the support and encouragement I have received from many individuals throughout the past years. Special thanks for the continuous mentorship and patience of my supervisor, Dr. Francois Tremblay. Thank you for wisdom, guidance and numerous character building opportunities provided over the project's development. I would also like to thank Janette Nason and Ben Smith for all of their continuous guidance, teachings and support in the laboratory during experimentations.

I would like to thank the members of my supervisory committee; Dr. Sarah Stevens and Heather Fennell-Al Sayed OC(C). Our discussions and suggestions helped pave the pathway to getting this project started. Thank you to the IWK Eye Care Team, and to the CVS program for encouraging me in both my research and my career as an Orthoptist. To my family, friends and colleagues at the Hospital for Sick Children for continuously giving me their encouragement and support throughout the project.

I would also like to thank the IWK Health Centre/Dalhousie University Clinical Vision Science Graduate Program NSHRF Scotia Support Grant Scholarship and NSERC Discovery Grant, who helped make this research possible.

CHAPTER 1: INTRODUCTION

Anesthesia is the temporary suppression of the nervous system using medications, causing loss of sensation/consciousness for pain prevention during medical procedures. There are a wide variety of agents used to create anesthesia, each having a different effect on analgesia (insensibility to pain), paralysis (inability to move), amnesia (loss of memory) and unconsciousness (state of not being awake). There is much known regarding the effect of anesthetic agents at the molecular level, specifically the interaction with channel receptors; however, the effect on the nervous tissue network is not as well understood. One clinical situation where the effect of anesthesia at the tissue level is important to consider is during diagnostic testing of the neurosensory retina. The retina is the light sensing tissue lining the back of the eye, making it difficult to examine without specialized instrumentation due to its posterior proximity. The most widely used methods of examining the retina involve ophthalmoscopy, which is used to inspect retinal morphology, combined with electroretinography (ERG), used to assess retinal function. The ERG is an objective technique for assessing retinal function that allows for detection and diagnosis of retinal abnormalities even in the early phases of diseases (Lin et al., 2009). The ERG is a compound field potential generated by various retinal cell types whose contributions depend on the stimulus used (Bui & Fortune, 2003). In younger children, or those with development delay, it is not uncommon to require sedation or general anesthesia during an ERG recording due to the length of procedure and conditions of testing. Effects of dissociative agents and general anesthetics on ERG signals are still controversial; however, previous studies have noted alterations to the normal patterns of ERGs while patients are sedated. These modifications make it difficult to interpret the signal, and make an appropriate diagnosis difficult (Tremblay & Parkinson, 2003). Alterations in ERG responses under anesthetic agents have also been documented in animal studies. The amplitude of ERG a- and b-waves in mongrel dogs were noted to vary when tested under different anesthetics (Lin, Shiu, Liu, Cheng, Lin & Wang, 2009). Larger a- and b-wave amplitudes were noted in scotopic ERGs and larger b-waves in

photopic ERGs of rats when sedated using katamine/xylazine; whereas selective inner retinal effects were noted in the ERG when sedated using isoflurane or urethane. (Nair, Kim, Nagaoka, Olson, Thule, Pardue & Duong, 2011).

In research, this becomes problematic as animal models, used for understanding the pathophysiology and for the development of new treatments, have ERGs under various forms of sedation/general anesthesia. The effects anesthetic agents have on retinal output during these procedures are still widely unknown. Anesthetics commonly used on smaller laboratory animals, Ketamine and Xylazine, will be used for this study. We will examine the effect of these substances on retinal ganglion cells activity, the cells that are downstream of the photoreceptors and bipolar cells in the visual pathway.

CHAPTER 2: ANESTHESIA

The technique of performing surgical procedures was dramatically improved in the 19th century with the introduction of general anesthesia, allowing for the development of modern surgery with the absence of consciousness, pain, and movement. In order to avoid adverse side effects and adapt to numerous procedures a combination of drugs such as hypnotics, muscle relaxants, analgesics, and sedatives are used (Grasshoff et al, 2006). The goal of anesthesia is to obtain amnesia, unconsciousness, analgesia and immobilization while maintaining physiological stability (Forman & Chin, 2008; Uhrig et al, 2014). Prior to 1846 Greek and Roman surgeons would use the effects of mandragora and wine to produce 'anesthesia' while preforming cutting or cauterization (Miller, 2010). Inhaled techniques, such as soporific sponges or alcohol fumes were reportedly used during surgery in the Middle Ages (Miller, 2010). Patients would often recall the surgical experience due to a lack of amnesia resulting in long-lasting emotional effects. Many patients with chronic ailments would often refuse surgical intervention for fear of the pain and high risk of death (Miller, 2010). In 1800, a young scientist named Humphry Davy wrote about his use of nitrous oxide and inhaled gas for the relief of pain caused by an erupting wisdom tooth. William Morton, initially trained as a dentist, was in search of an agent to relieve pain during denture fitting. He had observed demonstrations of nitrous oxide but ultimately performed his own experiments using ether and successfully administered the agent on September 30, 1846 for an upper bicuspid tooth extraction (Miller, 2010). Development continued with experimental use of Chloroform, nitrous oxide and fluorinated anesthetics (e.g. fluroxene), all with limited success. However, it was this public display showing that surgical intervention may be performed in the absence of consciousness, pain sensation, and movements that pioneered anesthetic practice (Grasshoff et al, 2006; Miller, 2010).

Today's definition of general anesthesia builds upon this stating that the agents reversibly produce amnesia, unconsciousness (hypnosis), and immobilization (Forman & Chin, 2008). These end points are produced by specific

interactions on discrete neuronal loci, which is in contrast to the historic hypothesis that there was a single global state change in the central nervous system (Forman & Chin, 2008). In order to understand the anesthetic end points of hypnosis and amnesia it is important to first understand the body's control of the arousal state (i.e. sleep) and how anesthetics effect these circuits (Miller, 2010).

2.1 REVIEW OF DIFFERENT MECHANISMS OF ANESTHETICS

Anesthesia is a state that shares phenotypic and neurobiological similarities with sleep. The active sleep hypothesis predicts that sleep is generated when specific neuronal systems increase their rate of firing, which causes the neural systems required for wakefulness to be inhibited. Baron Constantin von Economo hypothesized that there was a sleep-promoting region of the brain at the junction of the diencephalon and mesencephalon, near the optic chiasm (Constantinescu, 2000). In addition to this, there is a wake-promoting region in the posterior hypothalamus. This theory of active sleep has been strengthened through experimentation and with the identification of a population of inhibitory GABAergic neurons with state-dependent firing patterns, whose efferent projections inhibit wake promoting centers (Miller, 2010). During sleep and general anesthesia there is reduced responsiveness to external stimuli, thought to be due to anesthetic effects on the thalamus, resembling the natural thalamocortical inhibition seen in NREM (non rapid eye movement) state sleep (Brown, Purdon & Van Dort, 2011; Miller, 2010; Son, 2010). Within the thalamus there are reticular neurons and thalamocortical neurons that communicate with the cortex and integrate peripheral input. During anesthesia (& NREM sleep) reticular neurons are activated resulting in hyperpolarization of thalamocortical relay neurons, which blocks the action potential. Thalamocortical neurons are no longer able to relay peripheral input to higher cortical centers, thus temporarily separating the cortex from the periphery. Thalamic nuclei also receive input from the ascending brainstem reticular activating system as well as hypothalamic input from wake active centers (Brown, Purdon & Van Dort, 2011; Miller, 2010).

Anesthetic induced amnesia is likely due to the change in output of the hippocampus and amygdala in such a way that memory formation is diminished. Within memory formation there are three major themes: 1. There are multiple memory systems within brain regions that are sub served by specific neural circuits 2. There are multiple stages of memory formation mediated by molecular mechanisms 3. There is synaptic plasticity in memory storage (Miller, 2010; Son, 2010). The effects of anesthesia on consciousness may be explained by the disruption of information integration and the suppression of activity of the neural correlates at various levels of neural organization (Brown, Purdon & Van Dort, 2011). Consciousness reflects a higher integration of information by combining neural correlates of certain sensory modalities with other neural correlates (Brown, Purdon & Van Dort, 2011; Miller, 2010).

The important components for successful anesthesia include immobility, hypnosis and amnesia. Immobility, the depression of spontaneous or stimulus-induced movements, is the result of the anesthetic effect on spinal neurons (Grasshoff et al, 2006). Hypnosis is defined as unresponsiveness to verbal commands, whereas a deeper state seen in sedation includes features such as a decreased level of arousal, long response times, decreased motor activity and slurred speech. Amnesia is the term used to describe memory loss due to anesthesia. The loss occurs due to an effect on areas within the brain involved in transferring information from short term to long-term memory (Grasshoff et al, 2006). To achieve the goals of anesthesia a technique used is dependent on the procedure and depth of anesthesia required for a pain free experience. This can be achieved by inhaled or intravenous anesthesia. General anesthesia results in unconsciousness and is most often induced using intravenous drugs. Once induced a combination of agents including inhaled anesthetics, opiates, propofol, and neuromuscular blocking drugs are used for maintenance (Potyk, 1998). It is also important to note that the inhaled anesthetics have an additional system effect causing a decrease in arterial blood pressure by decreasing systemic vascular resistance, myocardial contractility, and stroke volume (Potyk, 1998).

Regional anesthetics provide anesthesia to more peripheral nerves and can be administered by spinal, epidural, intravenous, or peripheral nerve blocks. Local anesthetics are widely used for the treatment/prevention of acute pain, inflammation, cancer related pain, chronic pain, and also for some diagnostic purposes (i.e. topical anesthetics) (Heavner, 2007).

2.2 MOLECULAR ACTION

As mentioned earlier chloroform, ether and nitrous oxide were some of the first used agents in anesthesia, however they are all structurally different compounds (Grasshoff et al, 2006). In attempts to understand the mechanisms of anesthesia Meyer and Overton proposed 'lipid theories' in the 1900's , after they independently observed that the potency of an anesthetic increased proportionally to its oil/water partition coefficient (Franks, 2006). These theories suggest that most anesthetics are lipophilic, highly hydrophobic and alter the excitability of neurons by affecting the cell membranes (Uhrig, Dehaene & Jarraya, 2010). It's thought that the agents dissolved in the membrane are causing changes in the physiochemical properties, such as thickening of the cell membrane or structural changes in lipid bilayer (Grasshoff et al, 2006; Rudolph & Antkowiak, 2004). This mechanism was widely accepted for years; however, it implied the only structural feature of an anesthetic that was relevant was its lipophilicity (Grasshoff et al, 2006). The lipid theory fails to account for effects seen of optical isomers on proteins at different clinical concentrations (Grasshoff et al, 2006). In 1984, Franks and Lieb showed that anesthetics might work more specifically by inhibiting the function of a soluble protein (Uhrig et al, 2014). More recent theories focus on ion channels that are affected within clinical relevant ranges of anesthetic concentrations (Grasshoff et al, 2006).

The $GABA_A$ receptor (ϒ-aminobutyric acid) belongs to a superfamily of ligand-gated ion channels, and has been known to play the most important role as a functional site of general anesthetics (Son, 2010). They are a class of receptors that respond to the neurotransmitter GABA, an inhibitory neurotransmitter that reduced

postsynaptic activity (Grasshoff et al, 2006, Son 2010). These receptors are affected by a large number of anesthetic agents with effects seen at clinically relevant concentrations, and the action appears to follow the predictions of the Meyer Overton rule (Grasshoff et al, 2006, Son 2010). Once $GABA_A$ receptors, which are heteropentameric complexes composed of five different subunits, are activated there is an increase in cellular chloride and the cell membrane becomes hyperpolarized, resulting in a decrease in excitability (Son, 2010). Currently 19 subunits have been identified; however the most frequent combinations consist of α, β, and γ, with the ratio 2:2:1 (Son, 2010). It is the subunit configuration that determines the channels functionality and sensitivity to certain anesthetics (Son, 2010). At low to moderate concentrations general anesthetics enhance the effects of GABA on the $GABA_A$ receptor by increasing the inhibitory postsynaptic currents generated by the receptor. At higher concentrations the anesthetic may directly activate the receptor without the need for GABA (Son, 2010).

Another important target for anesthesia within the brain includes the N-methy-D-aspartate (NMDA) receptors. These receptors are activated by the neurotransmitter glutamate, a major excitatory neurotransmitter in the brain, and are highly distributed in the cortex, thalamus, striatum and brainstem (Uhrig et al, 2014). Glutamate receptors are ionotropic, comprised of four large subunits forming a central ion channel pore. Similar to other glutamate receptors, the NMDA receptor is a nonselective cation channel, allowing the passage of Na^+, K^+ and small amounts of Ca^{2+} (Purves D, Augustube GJ, Fitzpatrick D, et al. 2001). The presence of a co-agonist, glycine, and the removal of Mg^{2+} block at the channel during depolarization is required for the activation of the NMDA receptor and hence passage of the cations. There are different subunits of NMDA receptors (NMDA-R1 and NMDA-R2A through R2D) with different synapses being composed of distinct combinations of these subunits to produce a variety of NMDA receptor-mediated postsynaptic responses (Purves D, Augustube GJ, Fitzpatrick D, et al. 2001).

2.3 KETAMINE

Ketamine (2-O-chloro-phenyl-2methylamino-cyclohexanone, Ketalar®) is an anesthesic agent first synthesized and developed in the 1960's in search of a replacement for Phencyclidine (PCP, Angel dust, etc.), due to its abusive recreational usage. Ketamine is a dissociative anesthetic with analgesic properties at lower dosages (Wilcock & Twycross, 2011). Dissociative anesthesia is a unique form of general anesthesia that involves analgesia and amnesia but not complete unconsciousness. Subjects may still be able to swallow, keep their eyes open, and it is not uncommon to experience hallucinations, delirium or confusion while using the medication. Ketalar® is a racemic mixture of 2 enantiomers of equal quantity, S (+)-ketamine and R (-)-ketamine isomers which is the compound often used in veterinary anesthesia and experimental animal anesthesia (Mion & Villevieille, 2013).

The relatively high lipid solubility and low binding to plasma proteins allows rapid uptake of ketamine in the brain and a high bioavailability (%) through multiple routes of administration: intravenous, intramuscular, subcutaneous, trans nasal, rectal, oral, or an epidural (Potter & Choudhury, 2014). Oral routes of administration have been shown to result in a much lower bioavailability (approximately 17%), which is due to first-pass metabolism in the liver and gastrointestinal tract (Yanagihara et al, 2003). Nasal and rectal administrations for inducing anesthesia in children report a much higher bioavailability of 25-50% (Yanagihara et al, 2003). Sites of significant metabolism within the animal system include the kidneys, intestine, and the lungs (Mion & Villevieille, 2013). Ketamine is mostly metabolized into norketamine (80%), an active metabolite, due to oxidation by a microsomal enzyme system (Mion & Villevieille, 2013). There is additional metabolism of norketamine and three other metabolites are formed. Although norketamine is an active agent it only has one-third to one-fifth the activity compared to racemic ketamine (Potter & Choudhury, 2014). In humans the (S)-enantiomer of ketamine is four times more potent than the (R)-enantiomer (Yanagihara et al, 2003).

Ketamine interacts with many receptors both directly and indirectly with the most studied being the ionotropic glutamate receptor N-methyl-D-aspartate (NMDA), a channel closely involved in the development of dorsal horn neurons and the transmission of pain signals (Potter & Choudhury, 2014; Wilcock & Twycross, 2011). Ketamine acts as a non-competitive antagonist, inhibiting the channel-related flux of calcium and magnesium (Potter & Choudhury, 2014). Increasing the dose of the agonist (glutamate) will not overcome the antagonistic effects of Ketamine as the binding sites are different (ketamine binds in the NMDA receptor channel pore while glutamate binds to the extracellular surface of the receptor). The NMDA-glutamate receptor is blocked by magnesium when at rest. Once activated the channel is unblocked allowing calcium to move into the cell, resulting in neuronal hyper excitability (Wilcock & Twycross, 2011). Ketamine also interacts with other calcium channels, sodium channels, dopamine receptors, cholinergic transmission, and noradrenergic and serotoninergic re-uptake (Wilcock & Twycross, 2011).

Yanagihara et al. (2003) investigated the peak plasma concentrations of low dose ketamine administered to human volunteers by injection, tablet, sublingual tablet, suppository and nasal spray. Concentrations of ketamine were approximately between 50-100ng/ml up to one-hour post injection, declining exponentially after. The mean maximum concentration after the other modes of administration were 30-50ng/ml. Norketamine enantiomers were 35ng/ml for injection, 150-170ng/ml with the tablet, 90-100 sublingual tablets, 70-80ng/ml administered by suppository, and 30ng/ml by nasal spray. Psychotropic effects of ketamine have been reported with plasma concentrations ranging from 50-300ng/ml and with regional brain concentrations above 500ng/ml, with awaking from ketamine usually taking place at a plasma concentration in the range of 0.64- 1.12 μg/ml (WHO, 2006).

Ketamine exhibits clinical effects on many systems within the body. During anesthesia it acts as bronchodilator by stimulation of β_2 adrenergic receptors and by inhibition of vagal pathways producing an anticholinergic effect on bronchial smooth muscles. This differs from other anesthetics by preserving pharyngeal and laryngeal reflexes and maintaining the airway. There is also an increase in salivation, which may lead to airway obstruction. It also produces an increase in

blood pressure, stroke volume and heart rate making it less appropriate for use in animals with ischemic heart disease. Additional effects that could be associated with ketamine include, but at not limited to, an increase in skeletal muscle tone, increase in intraocular pressure and an increased serum rise in porphyric markers (Craven, 2007; Pai & Heining, 2007). Studies have looked into the use of ketamine as a glutamate receptor antagonist to prevent excitotoxicity within the central nervous system. Over stimulated NMDA receptors induce intracellular accumulation of free Ca^{2+}, inositol-1, 4, 5-triphosphate, diacylglycerol, and other compounds (Tsukahara et al., 1992). These chemical reactions are thought to play a part in the development of ischemic brain or retinal injury. Lower doses of Ketamine hydrochloride appeared to alleviate ischemic injury in the rabbit retina by the presumed method of antagonizing the NMDA receptor-mediated excitotoxic cascades. In contrast, higher doses of Ketamine appeared to impair retinal function (Tsukahara et al., 1992).

Within humans ketamine has psychic side effects, including changes in mood state and out-of-body experiences, which have been reported in adults and children upon wakening after ketamine administration. Animal studies measuring cerebral glucose levels have demonstrated that ketamine has a depressive effect on the inferior colliculus (acoustic relay nucleus) and the medial geniculate (visual relay nucleus). Garfield et al (1972) concluded that ketamine produces auditory, visual and proprioceptive confusion at a higher incidence compared to other anesthetics (Garfield et al, 1972, White et al, 1982). Investigators have also demonstrated ketamine's ability to have inhibitory and excitatory effects on the peripheral nervous system and central nervous system. Some animal study evidence showed ketamine to abolish epinephrine-induced arrhythmias in the heart by prolonging the relative refractory period (Idvall, 1979; White et al, 1982). Effects of ketamine have also been proposed at pre- and post- sympathetic ganglion receptors. In a guinea pig model, Juang *et al* (1980) found ketamine resulted in a depression of smooth muscle contraction in response to preganglionic stimulation and a transient increase in contraction to postganglionic stimulation.

2.4 XYLAZINE

Xylazine (Rompun®) is a α-adrenoceptor agonist typically used in veterinary practice as a sedative, muscle relaxant, and for its antinociceptive effects (Kanda & Hikasa, 2008; Veilleux-Lemieux et al, 2013). It was first developed in 1962 by Farbenfabrikin Bayer AG, Leverkusen in the Federal Republic of Germany for an intended use as an antihypertensive agent; however due to excessive CNS depressive effects it was then introduced into veterinary medicine to be used as a sedative (Greene & Thurmon, 1988).

Xylazine acts on the central nervous system by direct stimulation of alpha-adrenoceptors, which increases sympathetic discharge and reduces the release of norepinephrine (Greene & Thurmon, 1988; McIvor Road Veterinary Center, 1994). By blocking the release of norepinephrine there is subsequent bradycardia and reduced cardiac output (Silva-Torres et al, 2014). Similar to Ketamine, Xylazine is metabolized mainly by the liver and excreted by the kidney (Veilleux-Lemieux et al, 2013). Xylazine is extensively metabolized into many metabolites, with up to 70% of the dose eliminated in urine (Veilleux-Lemieux et al, 2013). The final breakdown of products are organic sulfates and carbon dioxide, with the main pathway of biotransformation being 1-amino-2, 6-dimethylbenzene; formed when the thiazine ring breaks down (Spyridaki et al, 2004). Pharmacokinetic data suggest that active drug is in fact xylazine, and not the resulting metabolites (Spyridaki et al, 2004).

Yasuhara et al. (2000), treated rats with 150mg/kg oral xylazine tablets. These rats showed symptoms of sensation and pain loss immediately with plasma concentrations reaching 2.88 μg/ml 1.5 minutes after consumption and slowly decline to 1.23 μg/ml 2 hours post ingestion.

In both the rat and human retina alpha-2α adrenergic receptors are located on the somas of the ganglion cells and many of the cells in the inner nuclear layer (Kalapesi, Coroneo and Hill, 2004). Other alpha-adrenergic receptor agonists are thought to work directly via interactions with their receptor as neuroprotective agents (Kalapesi, Coroneo and Hill, 2004).

Xylazine can cause decreased cardiac output during anesthesia. Decreased respiration rates have been observed in horses, but do not seem to have the same effect on cats and dogs (Greene & Thurmon, 1988). Other effects may include a decrease of tissue sensitivity to insulin (xylazine induced hyperglycemia), transient hypertension or hypotension.

CHAPTER 3: THE RETINA AS A MODEL

The retina is a thin piece of brain tissue lining the inside of the eyeball, made up of highly organized sensory neurons and intricate neural circuits that transmit the first stages of image processing to the optic nerve and brain for further visual processing (Kolb, 2004; Kolb 2006). It is an intricate structure assembled into 10 highly ordered layers (Figure 1); three of which contain the cell bodies of first, second, and third order neurons separated by layers of synaptic connections (Kolb, 2004; Nguyen-Ba-Charvet, 2014). The layers are designated, from outer to inner retina: retinal pigmented epithelium; photoreceptor cell layer; external limiting membrane; outer nuclear layer; outer plexiform layer; inner nuclear layer; inner plexiform layer; ganglion cell layer, nerve fiber layer, and internal limiting membrane.

3.1 RETINAL ORGANIZATION

The first layer, the retinal pigment epithelium (RPE), is an active area that functions as the blood-retinal barrier, selectively controlling the movement of substances from the choriocapillaries to the retina (Remington, 2005). The RPE is formed by a single row of prismatic cells containing melanin pigment, located within the cytoplasmic processes (Pycock, 1985). The RPE also carries out functions involved in the recycling of photoreceptor outer segments that are constantly shed, the storing and metabolizing of Vitamin A, as well as in absorbing light to reduced excess scattering (Remington, 2005).

The next section of the retina embodies the photoreceptors; beginning in the outer nuclear layer and expanding across the inner segment layers, synapsing with second order retinal neurons within the outer plexiform layer. There are two types of photoreceptors: rods are best equipped for low-light vision, and cones function best for daylight and bright colored vision (Kolb, 2006). These cells contain the photopigments that absorb quanta of light, the enzymatic machinery to transduce the activation of the photopigment into an electrical potential that is transmitted

through synaptic interaction to the next stage of integration/processing in the outer plexiform layer (Kolb, 1991). The external limiting membrane is the region of intercellular junctions between the photoreceptor cells and Müller cells. Müller cells are glial cells extending radially across the retina from outer and inner limiting membrane. They provide the architectural support for the retina, support metabolism, remove waste, and provide protection (Remington, 2005). The outer nuclear layer (ONL) is the layer of the retinal containing the cell bodies of the rods and cones. The nuclei of the cones are larger than those of the rods and thus the ONL is thickest in the fovea of the human retina where cones dominate (Remington, 2005).

The outer plexiform layer (OPL) contains the first area of synaptic connection in the retina found between the photoreceptors and bipolar cells (Kolb, 1991; Pycock, 1985). Rods and cones synapse upon various types of bipolar cells, different types of horizontal cells, in addition to cones passing information to one another and rods sending messages to cones (Kolb, 1991). The cell body of horizontal cells, amacrine cells, interplexiform neurons, Müller cells, and also some displaced ganglion cells are all found in the inner nuclear layer (INL) (Remington, 2005).

Axons of the bipolar cells and dendrites of the ganglion cells synapse in the zone called the inner plexiform layer (Pycock, 1985). It is within this layer that bipolar cells communicate with various amacrine cells and the dendrites of ganglion cells (Kolb, 1991). The message is then carried through the ganglion cell within the ganglion cell layer and finally into the nerve fiber layer, which consists of the ganglion cell axons (Remington, 2005). These axons project towards the optic disc to enter the optic nerve (Pycock, 1985). The internal limiting membrane is located between the retina and vitreous and is attached to fibers of the Muller cells, which penetrate the retina binding it together (Pycock, 1985).

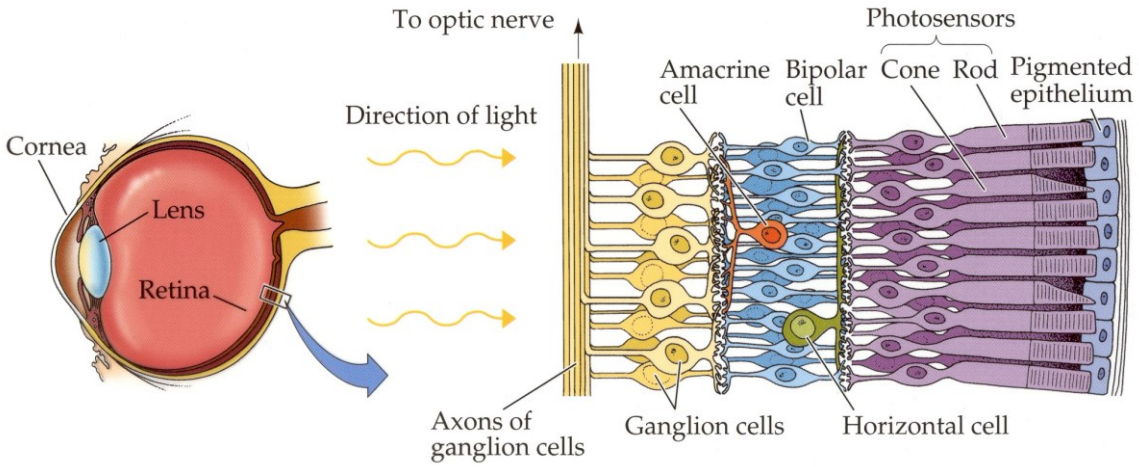

Figure 1. Schematic of the layers of the mammalian retina. Photons of light enter the eye and travel through the entire retinal thickness where they then activate the photoreceptors (rods and cones). The neural signal then travels to the bipolar cells and ganglion cells.

Note. From http://www.lifeinharmony.me/anatomy-of-eye-cones-and-rods/anatomy-of-eye-cones-and-rods-three-dimensional-retinal-ganglion-cell-google-search-totem

3.2 RETINAL PHYSIOLOGY/CIRCUITS

The transformation of light energy into a neural signal begins with the photoreceptors. The photoreceptors are composed of an outer segment, inner segment, cell body, and a synaptic terminal (Kevalov, 2011). The light sensitive photopigment, responsible for absorbing a photon of light, resides within the outer segment. Rods and cones differ in outer segment morphology: rods have a longer cylindrical outer segment, containing many disks; whereas cones have a shorter outer segment that tapers to a point, and contains fewer disks (Bear, Connors & Paradiso, 2007). This anatomical difference correlates with the functional difference in these two photoreceptors. With a higher concentration of photopigment, rods are over 1000 times more sensitive to light compared to cones, and thus contribute more to vision under scotopic (low light) conditions (Bear, Connors & Paradiso, 2007; Kefalov, 2011). This is in contrast to cones that do the majority of the work

during photopic (daylight) conditions. The function of these two photoreceptors is optimal due to the regional differences of their concentrations within the retina. The peripheral retinal contains a higher concentration of rods as well as a higher concentration of photoreceptor to ganglion cells, resulting in an increased sensitivity to light (Kevalov, 2011).

The visual process begins when light energy (photon) strikes the visual pigment found within the disk membrane of the photoreceptor. Within rods this pigment is called rhodopsin and can be thought of as a receptor protein (opsin molecule) with a bound chemical agonist (retinal), a derivative of vitamin A (Arshavsky, Lamb & Pugh2002; Bear, Connors & Paradiso, 2007; Pugh & Lamb, 2000). The opsin molecule has seven transmembrane alpha helices. Once a photon of light is absorbed there is a conformation change of retinal, activating the opsin molecule. This change begins a cascade then activating a G-protein (transducin), also found within the disk membrane, which then activates the enzyme phosphodiesterase (PDE) resulting in the breakdown of cyclic guanosine monophosphate (cGMP) (Arshavsky, Lamb & Pugh2002; Bear, Connors & Paradiso, 2007; Pugh & Lamb, 2000). Cyclic guanosine monophosphate is an intracellular second messenger continuously produced within the photoreceptor by guanylyl cyclase and acts to keep sodium (Na^+) channels open (Arshavsky, Lamb & Pugh2002). In darkness cGMP keeps the membrane potential of the rod outer segment depolarized by the steady influx of Na^+. The reduction of cGMP with the presence of light thus causes the Na^+ channels to close and the membrane potential to become more negative, resulting in hyperpolarization of the photoreceptor (Pugh & Lamb, 2000). As photopic conditions increase the cGMP levels within the rods decrease to a point where the response to light becomes saturated, resulting in no further hyperpolization (Bear, Connors & Paradiso, 2007). This is why vision during the day is dependent on the cone system. Cones react to photons similar to the process observed in rods; however, cone photoreceptors contain different opsin molecules within their disks. In humans cones contain one of three types of opsin molecules differentiated by the wavelength of light they are maximally activated by: Short wavelength (S-cone) or 'blue cones' are more sensitive to light with shorter

wavelengths around 430nm; medium wavelength (M-cone) or 'green cones' are sensitive to light around 530nm; and long (L-cone) or 'red cones' are most sensitive to longer wavelengths of light around 560nm (Bear, Connors & Paradiso, 2007). The difference in spectral sensitivity within the cones allows for the discrimination of color.

Similar to other neurons, photoreceptors release a neurotransmitter when depolarized (Figure 2). This is a counterintuitive process as light actually results in the release of fewer neurotransmitters. However, darkness is actually the preferred stimulus for a photoreceptor and thus when a shadow sweeps across it results in depolarization and neurotransmitter release (Bear, Connors & Paradiso, 2007). Once depolarized, neurotransmitters release glutamate from their synaptic terminals into the outer plexiform layer. Glutamate then binds to the dendrites of one of two classes of bipolar cells; ON-bipolar or OFF-bipolar (Jiulin & Xiongli, 1999). Within the outer plexiform layer bipolar cells also receive inhibitory inputs from GABAergic horizontal cells and glycinergic/dopaminergic interplexiform cells (Jiulin & Xiongli, 1999). OFF bipolar (ionotropic glutamate receptors) cells have glutamate-gated cation channels and depolarize with the influx of Na^+; ON-bipolar cells (metabotropic glutamate receptors) have G-protein-coupled receptors that respond to glutamate by hyperpolarizing (Bear, Connors & Paradiso, 2007). Typically there is convergence of synaptic connections from photoreceptors to bipolar cells. In addition to this, bipolar cells are connected via horizontal cells to a ring of photoreceptors (receptive field surround) that surround the central cluster, creating a receptive field (Bear, Connors & Paradiso, 2007). The response of a bipolar cell to light within the receptive field center is opposite to that of light in the surround (Figure 3). This antagonistic center-surround receptive field organization is passed on from the bipolar cells to the ganglion cells. Thus, when light activates the center of a receptive field an ON-center ganglion cell will depolarize, and an OFF-center ganglion cell will depolarize when there is a dark spot in the center of its receptive field. The response to center stimulation in both types of ganglion cells is antagonized when the surround is stimulated. For example: in an OFF-center ganglion cell the cells are hyperpolarized in the surround when a dark spot

stimulates the area, resulting in decreased firing of the neuron. However, when this dark spot moves and activates the center surround the cell increases its rate of firing. If the dark spot crosses and activates the center and surround simultaneously the rate of firing decreases but is still slightly different compared to baseline (i.e. light on).

3.3 RETINAL GANGLION CELLS AS PROBE OF RETINAL OUTPUT

Ganglion cells are important in the deconstruction of our visual experiences by using sequences of action potentials separated by periods of silence (spike trains), that travel down the optic nerve to higher cortical areas in the brain (Barry et al, 1997; Zeck & Masland, 2007). There have been many attempts to differentiate the sensory coding of ganglion cells including a classical characterization by qualitative descriptions of the responses (Zeck & Masland, 2007). The first attempt at using grating stimuli were conducted on simple cell types that possessed a simple receptive field structure. The response of these cells to laboratory stimuli can be predicted by static non-linearity and Poisson-like firing statistics (Zeck & Masland, 2007).

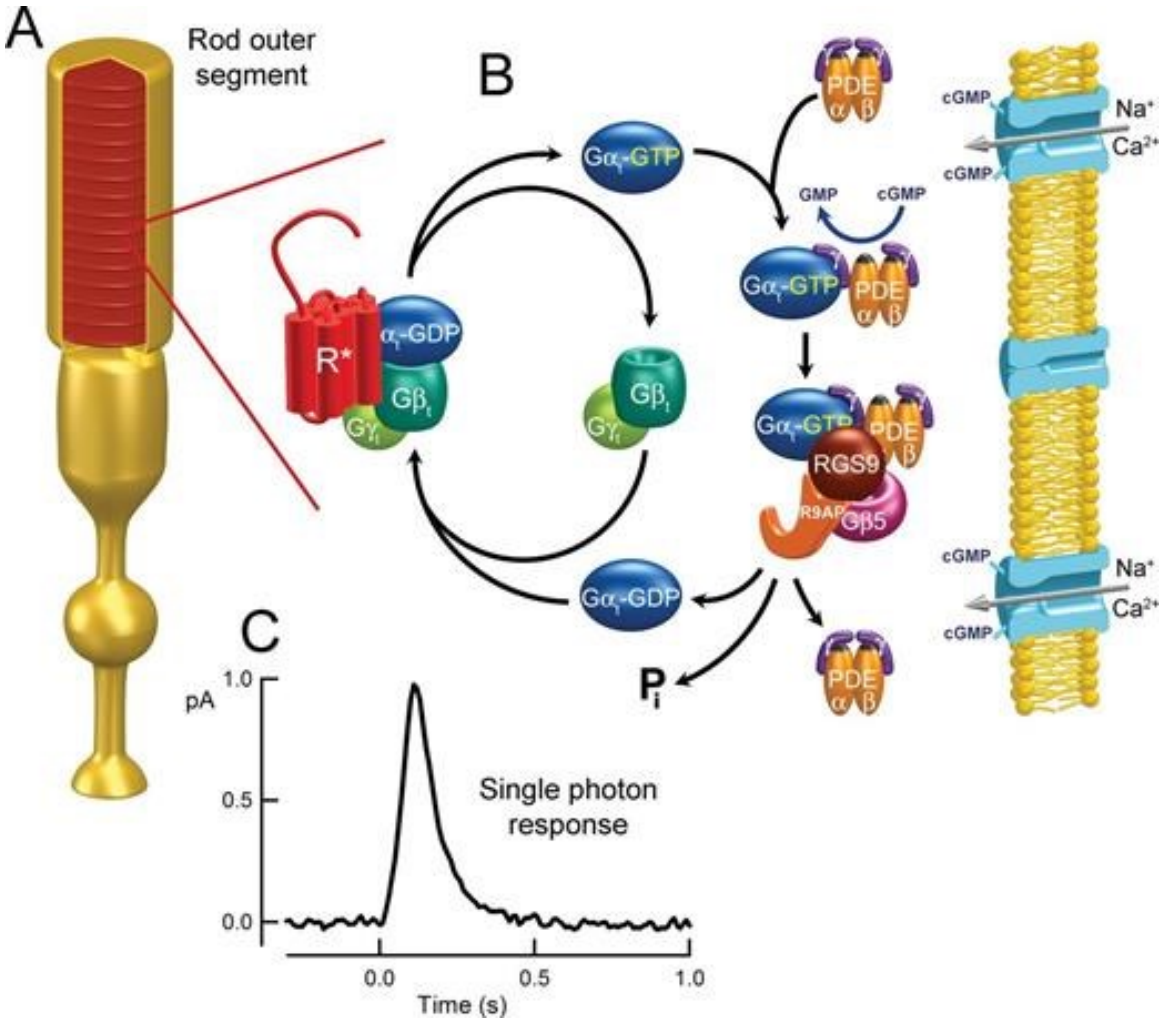

Figure 2. Phototransduction cascade of a rod photoreceptor in response to a light stimulus.

Note: From "Arshavsky, V.Y. & Wensel, T.G. (2013). Timing is Everything: GTPase Regulation in Phototransduction. Investigative Ophthalmology & Visual Science Vol. 54, 7725-7733.

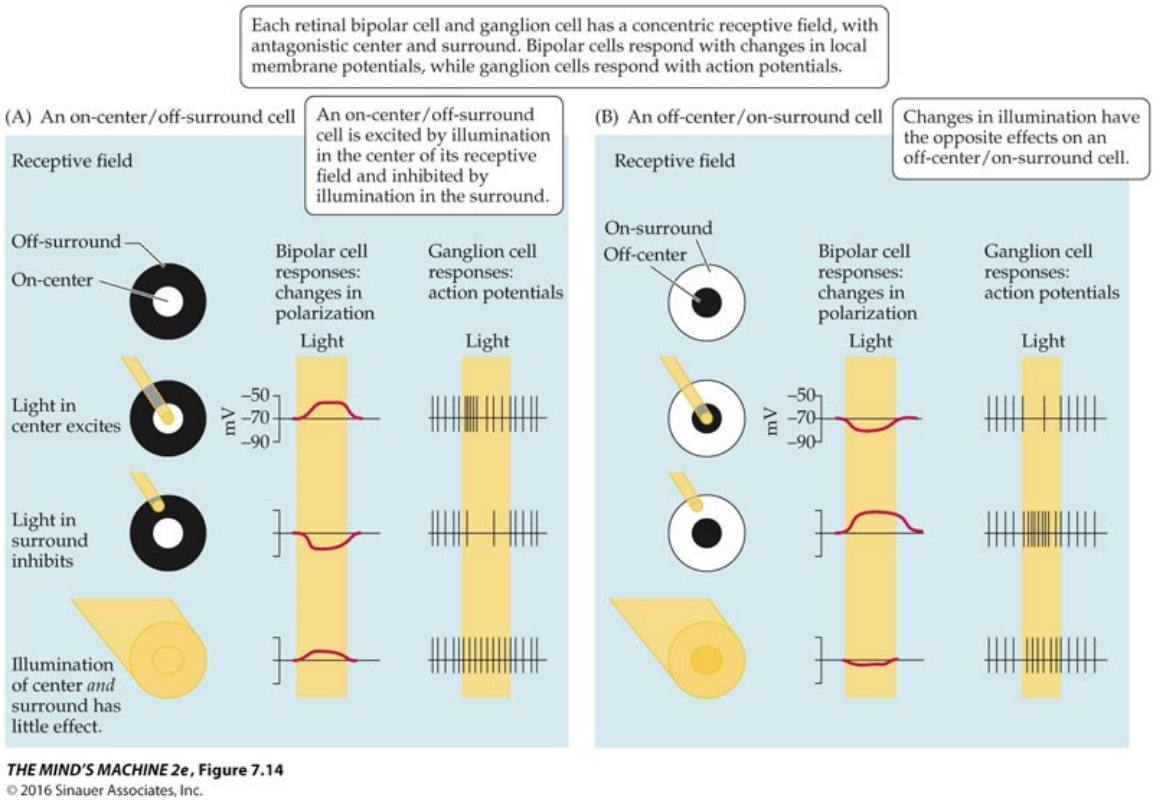

Figure 3. Schematic representation of antagonistic center-surround receptive field organization.

Note. From: "The Mind's Machine 2nd Edition, Foundations of Brain and Behavior. Chapter 7. Figure 7.14 Receptive Fields in the Retina. Textbook Reference: Neurons at Different Levels of the Visual System Have Very Different Receptive Fields, p. 188 Copyright 2015 Sinauer Associates"
https://2e.mindsmachine.com/figures/07/07.14.html

On average, spike count responses are reproducible, however they do display high variability. Within evoked conditions the spiking count variance over a set time window is closely proportional to the mean spike count, implying the variance to mean ratio is approximately constant as a function of firing rate (Moreno-Bote, 2014). This variance to mean ratio constancy is a property of the distribution of a neuronal population but also for every single neuron in the population. This

property is referred to as Poisson-like firing, in analogy to the Poisson process where the variance to mean ratio is rate independent (Moreno-Bote, 2014).

Retinal ganglion cells generate more spikes than their geniculate targets (Rathbun et al, 2007). One important factor in determining if a retinal spike will trigger a geniculate spike is the retinal interspike interval (ISI). Shorter ISIs have the greatest efficacy for generating postsynaptic action potentials, whereas longer ISIs decrease progressively until there is no detectable influence of ISI on the production of postsynaptic spikes (Martiniuc & Knoll, 2012; Rathbun et al, 2007). Using multielectrode array technology Zeck and Masland (2007) were able to distinguish ganglion cells into different cell types by the temporal pattern of spiking activity. They classified them as either ON and OFF transient, ON and OFF sustained, uniformity detectors, ON direction selective cells, local edge detectors and the four ON-OFF direction selective cell subtypes. They defined the action potential as the first spike (cardinal) of a coding event if it was preceded by a period of silence longer than the an arbitrary time (T) and if the following spike occurred within the time interval T. Once the ISI exceeded the threshold T their coding event was considered complete. This can be visualized in (Figure 4) using an ISI map where each spike is represented as a function of both the preceding and the following ISI (Zack & Masland, 2007). Within the lower right quadrant of the figure the cardinal spikes show a shallow shape indicating that the second spike in an event occurs very soon after the cardinal. In the lower left quadrant the spikes occur between the cardinal spike and the final spike of the coding event, and the upper left represents the terminal spike in the coding event (Zack & Masland, 2007).

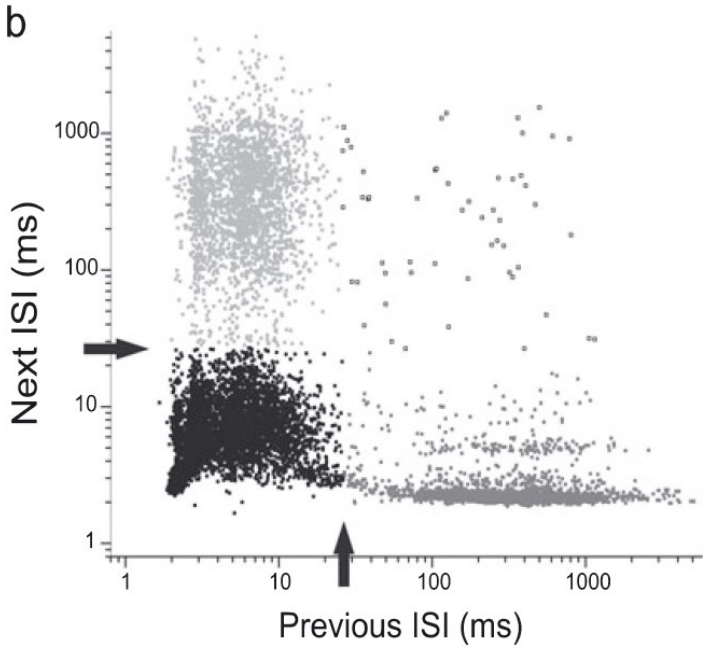

Figure 4: Joint interspike interval (ISI) plot for the spike train of an ON_OFF DS cell in response to spatial white noise. For each spike a point is plotted showing the duration of the preceding ISI and the duration of the subsequent ISI. In this plot four areas are distinguishable, which are used to define coding events; the spikes in the lower right quadrant (dark gray) represent the first spikes in a coding event, the spikes in the lower left quadrant the intermediate spikes (black dots) and the spikes in the upper left corner the last spikes in an event (light gray). Spikes in the upper right quadrant represent solitary spikes, which are preceded by a long interval and also followed by a long interval.

Note. From "Zeck, G.M. & Masland, R.H.(2007). Spike train signatures of retinal ganglion cell types, Figure 2b. European Journal of Neuroscience, 26, 367-380."

3.3.1 MULTIELECTRODE ARRAY TECHNOLOGY

Multi-electrode arrays (MEAs) are electrophysiological tools consisting of dozens to thousands of electrodes, allowing for measurements of many neurons in parallel (Reinhard et al, 2014). The layered structure of the retina, with its many

circuits makes it an ideal tissue for MEA experimentation. Unlike other neuronal tissues, such as those found within other brain networks, the retina may be placed flat down on the MEA untouched as most retinal ganglion cells are present and accessible. Ex-vivo experimentation entails the extraction of retinal tissue from the eye, which is then placed ganglion cell side down on the electrodes (Figure 5). Light stimulation is then applied from above or below the MEA (if transparent). Photoreceptors capture light, which is then processed by retinal circuits resulting in ganglion cell spike generation. The MEA measures these spikes as voltage changes (Reinhard et al, 2014). Algorithms are then used to match multiple spike patterns to the raw data obtained. Each ganglion cell produces a pattern of activity that is driven by its unique synaptic inputs. Standardized peristimulus time histograms (PSTHs) are constructed to characterize the rate and timing of the retinal ganglion cell action potentials in relation to the light stimulus presented. Spiking activity captured by the MEA is recorded first over a set number of sweeps which is then saved and windowed. PSTHs are generated for individual cells within a defined bin width. This data can be used to count the total number of spikes in individual bins prior to, during and after the stimulus is presented.

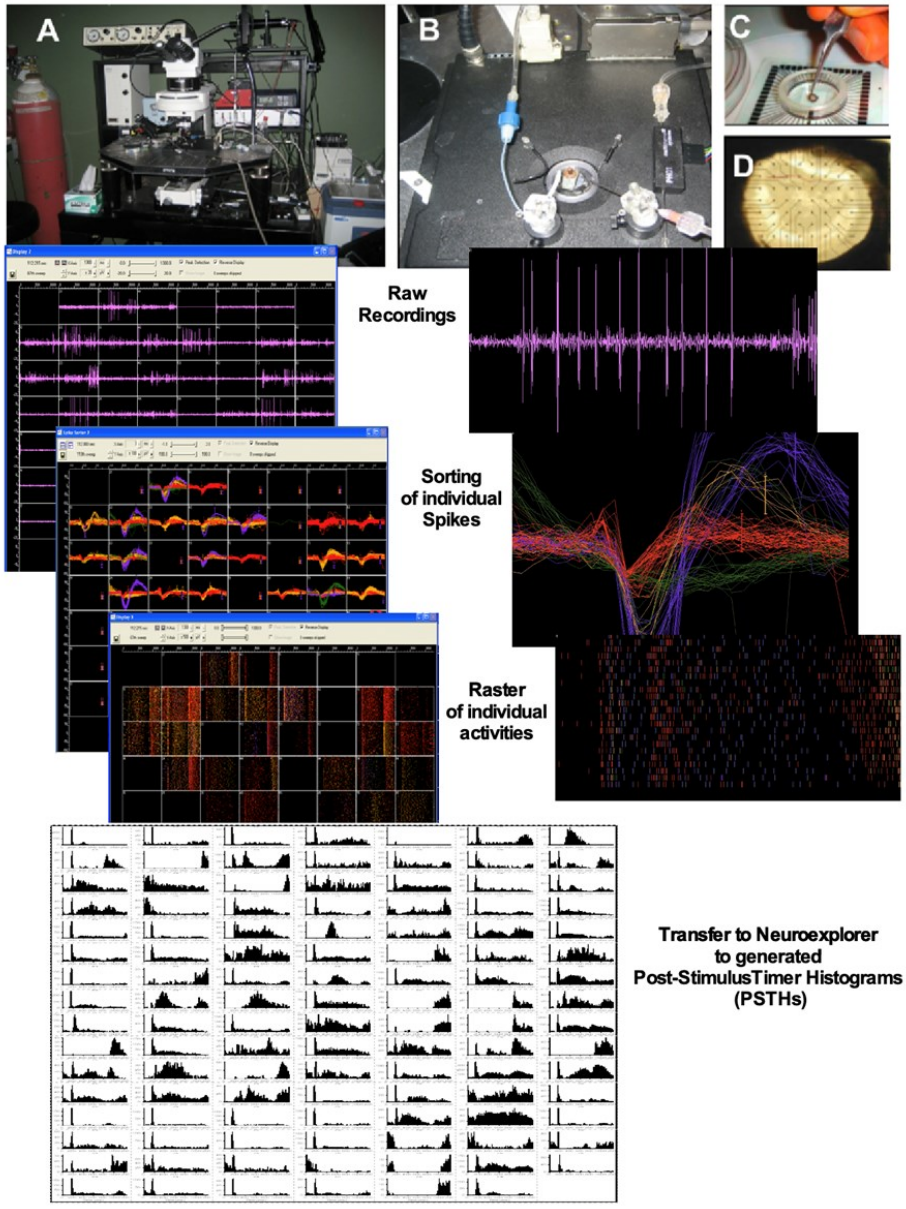

Figure 5. Multi-electrode Array System. Full view of system (A) with CO_2 chamber on left, microscope centered, light stimulus projection from below microscope, perfusion system to the right of photograph. The retinal preparation mounted on MEA slide over light stimulus with prefusion drips (B). The multi-electrode array electrode plate with retinal preparation mounted on filter paper (C). Inferior view of MEA plate with electrodes highlighted (D). Raw recording examples of spiking during experimentation, spike sorting software and peristimulus time histograms (PSTHs) used for cell classifications.

CHAPTER 4: GUINEA PIG AS AN ANIMAL MODEL

Altricial animals, those born with their eyes closed, such as rats and mice, are most widely used in experimental electrophysiology. Both the anatomy and physiology of their retinas differ from precocial animals, such as guinea pigs and primates (humans), which have their eyes open at birth.

Rodents are nocturnal animals with predominantly rod-dominated retina. The retina of rats and mice are composed of only 1.5% and 3% cones, respectively. The Guinea pig, which has traditionally been classified as a rodent, actually has an ordinal status separate from *Rodentia,* based on recent phylogenetic analysis (Lei, 2003). These diurnal animals have a larger percentage of cones (8-17%) in the retina, more similar to the 6% reported in human subjects (Racine et al, 2005). Electroretinogram studies have identified two classes of cones within the guinea pig retina with peak sensitivities of 429 (S-cone) and 529nm (M-cone), indicating the basis for color discrimination (Lei, 2003). These findings are different than those of rats and mice, which have an ultraviolet (UV-cone) with a spectral sensitivity of 360nm and a second cone type photopigment around 510nm (Lei, 2003). In addition to this guinea pigs have both axon-less and axon-bearing type horizontal cell organization, implying inner retinal organization for more complex cone vision. In contrast, rodents only have axon terminal systems connecting to rod photoreceptors (Lei, 2003). Axon-less (A-type) horizontal cells have larger, more branched dendritic trees and connect exclusively with cones. Whereas axon-bearing (B-type) horizontal cells have smaller dendritic trees, and an axon ending in a profuse axon terminal system (Peichl & Gonzales-Soriano, 1994).

The scotopic ERG responses in rodents (mice/rats) and guinea pigs are similar to those of humans, while photopic responses are quite different in rodent models. The photopic response of rats and mice do not include an easily measurable a-wave, and the b-wave is larger in amplitude compared to those found in human subjects (Racine et al, 2005). The ERG of the guinea pig shares similarities to that of humans, including: a-wave, b-wave, OP composition, and the photopic hill phenomenon (Racine et al, 2005; Wood et al, 2010). The photopic hill phenomenon

describes the characteristic increase in the amplitude of the b-wave to a maximal point with increased luminance. After this point there is a decrease in amplitude as the luminance continues to increase. A positive OFF component during a photopic long flash, demonstrated by Lei (2003), is an additional similarity of the guinea pig and human retina (Wood et al, 2010).

Altricial animals are born with an immature visual system with the retina typically composed of only two nuclear layers: the inner (ganglion cells) and outer (undifferentiated neuroblastic cells) (Racine, 2008). There are significant architectural changes throughout the retinal accompanying eye opening, which is usually during the second week of life. As a result of this the retina is not functionally mature until the end of the first month and an electroretinogram cannot be recorded from birth. In contrast to these findings, the retina of precocial animals matures in utero and is well developed at birth. Racine et al, 2008 investigated both the structural and functional maturation of the Guinea pig retina. They found Guinea pigs, like other precocial animals described in the literature, were born with nearly adult-like photopic and scotopic ERGs. There was significant age-dependent architectural reorganization of retinal tissue within most layers, which were not correlated with the normal growth of the eye. However, even with these structural changes the ERG reflected amplitude and peak time changes, which is suggestive of a maturation process, also seen in human subjects.

The structure of the guinea pig retina is similar to humans, aside from an overall thinning of each layer; however the transport of oxygen differs significantly due to differences in retinal vasculature (Yu & Cringle, 2001). The guinea pig retina is completely avascular and the oxygen delivery is provided by choroidal circulation. This differs significantly from the human retina that delivers oxygen to the outer retinal layers through a choroidal circulatory system and oxygen to the inner retinal layers via retinal circulation (Cringle et al, 1996; Wood, 2010). Yu and Cringle (2001) obtained oxygen profiles in the avascular guinea pig model under normal air breathing conditions and found that oxygen diffusion distance does not limit retinal thickness and that much of the inner retina survives essentially within an anoxic environment. This represents an advantage to using the guinea pig retina on the

MEA as the oxygen supply during experimentation is only possible via tissue diffusion.

CHAPTER 5: METHODS

5.1 PROTOCOLS

The effect of Ketamine, Xylazine, and a combination of the two anesthetics on the guinea pig retina were conducted *ex vivo*. To quantify the impact on the retina, retinal ganglion cell (RGC) action potential activity was monitored and compared at baseline, after administration of the anesthetic(s), and during a recovery phase.

The retina was collected from the guinea pig eye cup and placed ganglion cell side down in the perfusion chamber of the 8X8 multielectrode array (MEA) (30μm electrode diameter, 500μm spacing), maintained at a temperature of 36 degrees. The specimen was then perfused with Ames solution to maintain viability and stimulated with a variety of long-duration light stimuli (LED 530nm, 1000ms, 400 lux). The electrical activity from the retina was recorded by the MEA and then windowed in order to isolate RGC spiking activity. After this baseline recording Ketamine, Xylazine (or the combination of the two anesthetics) was administered within a solution of Ames into the perfusion system, at various concentrations. Following recording of the active drug a washout phase of Ames solution perfused the retina to measure RGC spiking after recovery. The spiking counts of each drug assay were determined using spike sorting software. The viability of the *ex vivo* preparation was tested by Wood (2010). After a 2.5 hour period of perfusion on the MEA there was no significant decrease in spontaneous RGC spiking activity triggered when a light stimulus was turned ON and OFF.

5.2 ANIMAL PREPERATION

All animal care including euthanasia adhered to the Canadian Council on Animal Care standards, as well as those pertaining to animal research at Dalhousie University. Hartley guinea pigs were euthanized with Euthanyl (100mg/kg

pentobarbital; Bimeda-MTC, Cambridge ON) in accordance with the weight of the animal and then quickly sacrificed by cervical dislocation to prevent too strong contamination of pentobarbital on the retinal preparation. On animal death, the eyes were removed by first elevation of the globe with forceps, followed by the cutting away of extraocular muscles, conjunctiva, and surrounding tissue. Finally, the optic nerve was severed and the globe transferred to a petri dish filled with Ames' solution at room temperature. The eye was then perforated with a scalpel at the ora serrata and micro-scissors were used to cut around the circumference of the limbus to remove the anterior segment of the globe. The eyecup was then placed in Ames' solution, contained within a mesh-lined basket, and perfused with CO_2 for approximately 10 minutes to theoretically help facilitate the detachment of the vitreous from the retina. After 10 minutes one eyecup was removed while the second eyecup was kept as a spare. The vitreous was then removed from the eyecup by means of forceps and small paintbrushes to exercise great care in avoiding retinal tearing. The retina to be used was then gently brushed away from the choroid by use of the soft tipped paint brush, cut to an appropriate size and placed ganglion cell side up on a piece of filter paper (Millipore, Billerica, MA). The filter paper had a precut central hole to allow more perfusion of solution to the retina throughout experimentation. All edges of the retina were flattened down onto the filter paper by means of the brush and then the preparation was placed RGC side down onto the MEA (heated to 37^0C) and immediately re-perfused with Ames solution. The preparation was allowed 10-15 minutes of perfusion before spiking activity was subjectively stable before experimentation began.

5.3 PERFUSION SYSTEM

The Ames' solution was made by adding 1.9g of sodium bicarbonate to 1 liter of distilled water and then bubbled with carbon dioxide (CO_2) for 10 minutes. One bottle of Ames' medium (8.8g/L; Sigma-Aldrich, St Louis, MO, USA) was then added to the solution and maintained at a pH of 7.4, measured with a pH meter (Denver Instruments GmbH, Göttingen, Germany). Adjustments were made with the addition

of sodium hydroxide (1N) or hydrochloric acid (1N) until pH remained stable. The solution was then placed into a heating bath to maintain the temperate at 37^0C and bubbled with CO_2 to avoid precipitation of calcium carbonate ($CaCO_3$).

The methodology of perfusion was adopted from Wood (2010). The perfusion chamber (diameter of 26mm; height 3mm) was attached centrally around the MEA, surrounding the area of which the retina was placed. Within the chamber, a stainless steel harp (SDH-26H10, Harvard Apparatus, St.Laurent, Canada) was placed on the retina (with filter paper) and additional weights if needed, in order to minimize the movement of the sample with perfusion. A Miniplus 3 peristaltic pump (Gilson, Inc., Middleton, WI) was used to pump the Ames' solution through polyethylene tubing (1/16 inch diameter) into the retinal chamber. A dripper made of a syringe needle and pipette tip, removed from the chamber via thin tubing; which was also connected to the peristaltic pump. The speed was adjusted in order to maintain a depth of perfusion of 0.1mm below the surface. A silver-silver chloride (Ag/AgCl) grounding electrode was then placed within the chamber, making contact with the solution.

Ketamine was prepared from a solution of Ketalar® 100mg/ml. Ketamine was diluted in Ames's solution to a low doses of 0.01mg/ml (10,000 ng/ml), 0.05mg/ml (50,000 ng/ml), 0.1mg/ml (100,000 ng/ml), 0.5mg/ml (500,000 ng/ml) and a high dose (0.5mg/ml-1.0mg/ml). The ketamine solutions were maintained at the same temperature and pH as the Ames's solution. Once the retinal preparation was placed on the MEA it was perfused with Ames's solution and allowed to stabilize (~5-10 minutes). Once spiking behavior appeared stable a baseline recording was captured (60 sweeps) for each light stimulus. The ketamine solution was then administered and allowed to perfuse the retina for 5-10 minutes and spiking activity was recorded again for each light stimulus (60 sweeps). The retina was then perfused again with Ames' solution (20-30 minutes) and recovery recordings to each stimulus (60 sweeps). The recovery recordings were used for the baseline of the next concentration and the methods repeated. Multiple concentrations were used on each retinal preparation to limit the amount of guinea pig sacrifice.

Xylazine was prepared from a solution of Rompun® 20mg/ml. Xylazine was diluted in Ames's solution to dosages of 0.0004mg/ml (400 ng/ml), 0.004mg/ml (4,000 ng/ml), 0.04mg/ml (40,000 ng/ml) and 0.4mg/ml (400,000 ng/ml). The solutions of xylazine were maintained at the same temperature and pH of the Ames's solution. The same protocol of spike recording was followed as with ketamine.

To evaluate the effect of a combination of the two drugs a concentration of 0.01mg/ml (10,000 ng/ml) ketamine was administered after baseline, spiking recorded and recovery as in previously mention protocols. The recovery recordings of Ketamine 0.01mg/ml were the baseline for the combined mixture of Ketamine 0.01mg/ml and Xylazine 0.004mg/ml.

Table 1: Blood plasma levels sampled of ketamine and xylazine, after drug administration at various anesthetic and sub-anesthetic dosages in human and animal models.

Dose, route, species	**Plasma concentration**	**Reference**
Ketamine 237.7 g/mol		
9 mg/kg, IV Children 2-9 y.o.	500-2000 ng/ml	Malinovsky et al (1996)
250 mg/kg, IV adults	200 ng/ml	Clements & Nimmo (1981)
2mg/kg, infant	320 to 437 ng/ml	Saarenmaa et al (2001)
1125mg/kg, rats	4000-10000 ng/ml	Veilleux-Lemieux et al (2013)
NA	2000 ng/ml	Niedorf et al (2003)
25mg (tablet), adults	150-200 ng/ml	Yanagihara, Y. et al. (2003).
50mg (sublingual tablet)	100 ng/ml	Yanagihara, Y. et al. (2003).
20mg injection	100-1000 ng/ml	Yanagihara, Y. et al. (2003).
Xylazine 220.3g/mol		
NA	600-1000 ng/ml	Veilleux-Lemieux et al (2013)
NA	150 ng/ml	Niedorf et al (2003)
1.4 mg/kg, IV dogs	500-1000 ng/ml	Garcia-Villar et al (1981)

5.4 MEA RECORDING

A standard multielectrode array (Multi Channel Systems, Reutlingen, Germany) containing 60 electrodes, made of titanium nitride, in an 8X8 layout grid

was used (Figure 6). The electrodes were 30μm with an interelectrode spacing of 500 μm. The MEA sensor was placed on the MEA preamplifier with blanking circuit (MEA-1060-BC-PA, Multi Channel Systems MCS GmbH, Reutlingen, Germany). The contact pins in the lid of the amplifier are pressed onto the contact pads of the MEA. The signal was then sent to the MEA filter amplifier with a gain of 1000 and bandwidth ranging from 0.1Hz-10kHz. The amplifier emitted a signal to the data acquisition computer by means of a 68 pin MCS standard cable. The MEA system has a 50kHz sampling rate per channel. The analog output signals of the MEA amplifier are then acquired and digitized by the MC card. In addition, the MEA amplifier also comes equipped with an integrated heating system that maintained the temperate of the MEA and was programmed by a temperature controller (Multi Channel Systems MCS GmbH, 2005; Wood 2010).

Prior to testing the MEA was stored in distilled water at room temperature and cleaned prior to each use by being placed in an ultrasonic cleaner (L&R Manufactoring, Kearbsay, NJ) with Teragazym detergent (Alconox, White Plains, NY), followed by a thorough rinse of distilled water.

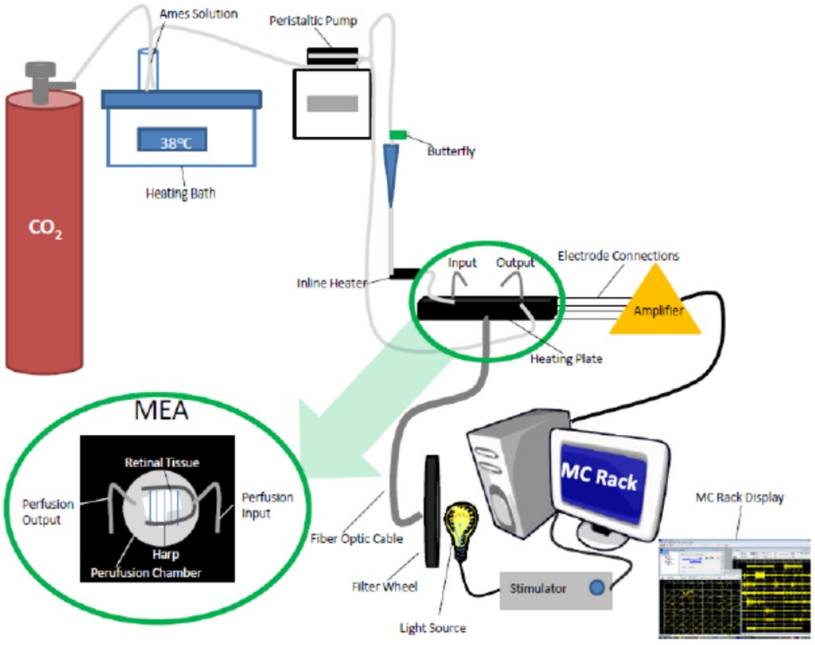

Figure 6. Schematic of the MEA set-up. A peristaltic pump delivers Ames solution, which was previously bubbled by CO_2 tank and heated to 37^0C, to the retinal preparation. MEA sits on a heating plate maintained at 37^0C (outlined in green). The retinal preparation sits ganglion side down with a harp sitting on top to prevent movement during perfusion of solution. Electrodes of the MEA connect to an amplifier that delivers the electrical output of the retina to the MC Rack software on the computer. Filter wheel is used to control light intensity from the light source illuminating the retina via a fiber optic cable.

Note. From "Wood, L. (2010). Regulation of retinal activity in an ex-vivo guinea pig model by experimental conditions and effects of isoflurance and propofol anesthetics. Dalhousie University Master of Clinical Vision Science Program, 1-112."

5.5 SPIKE SORTING/FILTERING

Raw electrode data was recorded and stored on the computer hard drive using MC_rack software (Multi Channel Systems MCS GmbH, Reutlingen, Germany). The replayer function of MC-rack software was used to retrieve data from each

experiment and isolate RGC spiking activity by means of a high pass and low pass filter. Spiking activity was differentiated from baseline noise within the software by setting thresholds for each individual electrode. A windowing function was then used to isolate individual RGC cells and a raster plot for the activity captured by individual electrodes was also created. The output file with filtered RGC action potentials was recorded and imported to Neuroexplorer software (Nex Technologies, Littleton, MA) for further analysis (Wood, 2010).

5.6 PSTH DESCRIPTION

Standardized peristimulus time histograms (PSTHs) were created to characterize the rate and timing of RGC action potentials in relation to the light stimulus. The RGC activity was recorded over a set number of sweeps (60) and windowed/ saved using MC_rack software, then imported into Neuroexplorer software. The PSTHs were created for individual cells using a bin width of 0.1s for numerical analysis and then subsequently exported into Microsoft Excel. Within excel the total number of spikes in individual bins were combined so spike counts could be calculated for 300ms before the light stimulus, while the light stimulus was ON and while the light stimulus was OFF (Figure 7).

5.7 CELL CLASSIFICATION

Cell status was classified based on average spontaneous (pre-stimulus, stimulus on and post stimulus) cell spiking activity. Low activity cells were assigned to those RGCs firing up to 500 times within the 300ms window. Intermediate activity cells were assigned to those RGCs firing between 500 to 1500 times within the 300ms window. Finally high activity cells were assigned to those RGCs firing at a rate higher than 1500 within the 300ms window (Figure 7).

The status of a cell was labeled according to first control of an experiment and carried through (status of a single cell can change, going from tonic to inter to phasic after several ketamine assays).

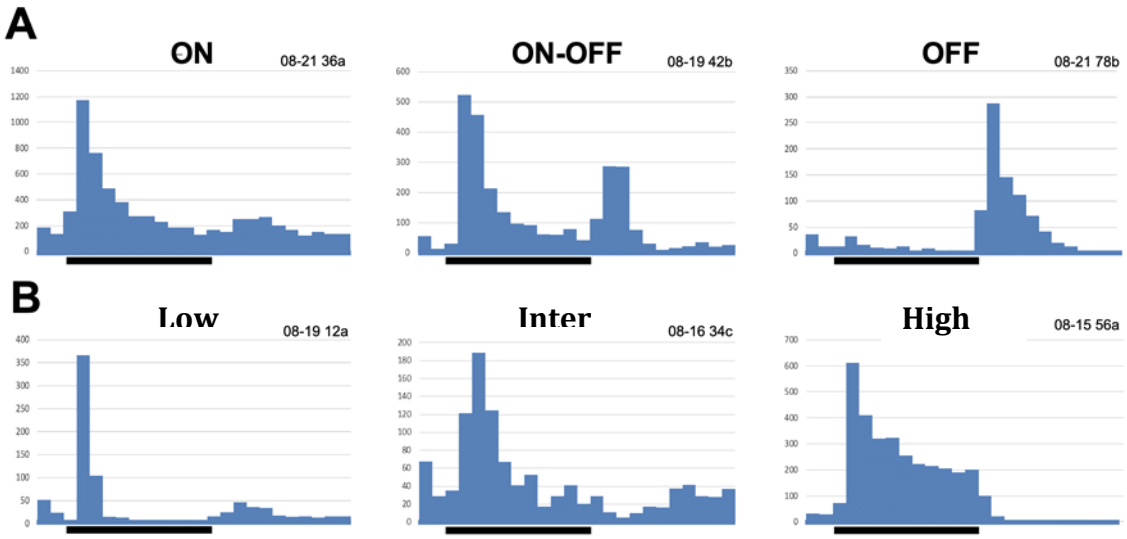

Figure 7. Retinal ganglion cell firing patterns.
(A) RGCs responding to light stimulus ON (left); light stimulus OFF (right), and mixed response (center). (B) Low activity RGCs (left), intermediate (center), and high (right). Number of ganglion spikes (frequency) over time (ms); light stimulus onset and duration indicated by black bar (300ms onset, 1000ms duration).

5.8 COMPILATION OF RATIO

To compare any effects of the drug(s) on RGC spiking, a ratio of spiking activity at baseline (recovery of previous experiment) to spiking activity after retinal preparation was exposed to specific drug concentration was used. Using Microsoft® Excel® (Microsoft Excel 2010 ©Microsoft Corporation) averages of spiking for low, intermediate and tonic activity type cells were calculated. As discussed previous the cell classification was determined by cell firing behavior, during the entire recording window. Each RGC spiking window was compared to the spontaneous spiking at the beginning of the experiment; on subsequent drug concentrations the baseline was considered the recovery recording of the previous concentration. The ratio was calculated for the overall spiking (300ms prior to stimulus, 1000ms of stimulus onset, and 900ms post stimulus) as additionally

broken down to compare ON responses (within 1000ms of stimulus) and OFF responses (900ms post stimulus). The average ratio for each condition was then calculated for each drug concentration.

5.9 STATISTICAL ANALYSIS

Microsoft® Excel® was used to graph global effects of drug concentration on total retinal spiking in additional to retinal spiking of low, intermediate and high activity cell types. The response was further broken down into cell response to capture changes in spontaneous activity (300ms prior to light stimulus), ON and OFF responses. The RGC firing patterns were assessed to see if the cell behavior changed during exposure to the drug. To assess this a percentage change calculation for the global retina was done setting our expected Phasic behavior ratio to be 0.8, Intermediate >0.8 to <1.2, and Tonic >1.2.

Data was then log transformed, transferred to SPSS (IBM SPSS Statistics) and a one-way multivariate analysis of variance (one-way MANOVA) was used to determine whether there were any effects amongst cell types and drug concentrations. Differences in mean RGC spiking ratios were also assessed using a one-way ANOVA for each cell type (low activity, intermediate and high) across the different concentrations of ketamine and again for xylazine. At each anesthetic concentration a t-test was conducted to see if the ratio of mean RGC spiking varied across total cell spiking, spontaneous activity, ON responses and OFF responses.

CHAPTER 6: RESULTS

6.1. KETAMINE

6.1.1 GLOBAL EFFECT ON SPIKING RATIO

Peristimulus time histograms, sum of all cell activity recorded on the MEA, were created by averaging spiking activity across the duration of the light stimulus. These values were then normalized to allow for inter cell variations. The histograms show the spontaneous activity prior to the onset of the stimuli, the responses during the flash and cell responses directly after the flash. A long duration flash was used to separate ON from OFF components. The amount of cell spiking did not appear to show a significant reduction; however there seemed to be a shift in when the cells were spiking (Figures 8.1 and 8.2) as the concentration of ketamine increased.

There was an increase in the mean spiking ratio of all ganglion cell responses (including spontaneous activity, ON and OFF response) in the experiment compared to baseline for each concentration of ketamine administration, except for the reduction in the ratio seen for the highest concentration of ketamine (Table 2). The greatest increase in spiking ratio was seen in ketamine 0.05mg/ml, however this concentration also shows the highest variance.

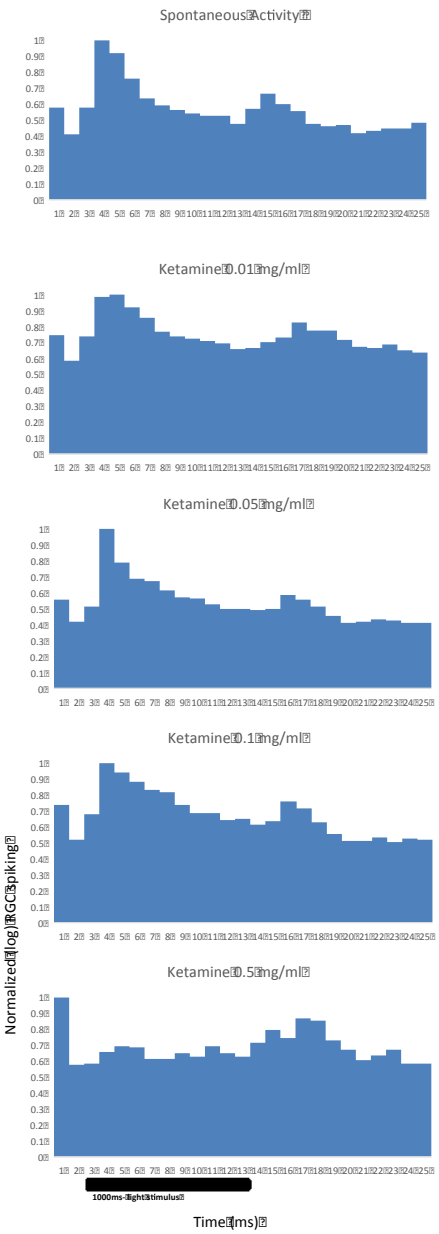

Figure 8.1. Peristimulus time histogram of average RGC spiking activity (frequency) over time (ms) at multiple concentrations of ketamine.
Normalized (log transformed) data; black bar indicating 1000ms of light stimulus onset beginning at 300ms.

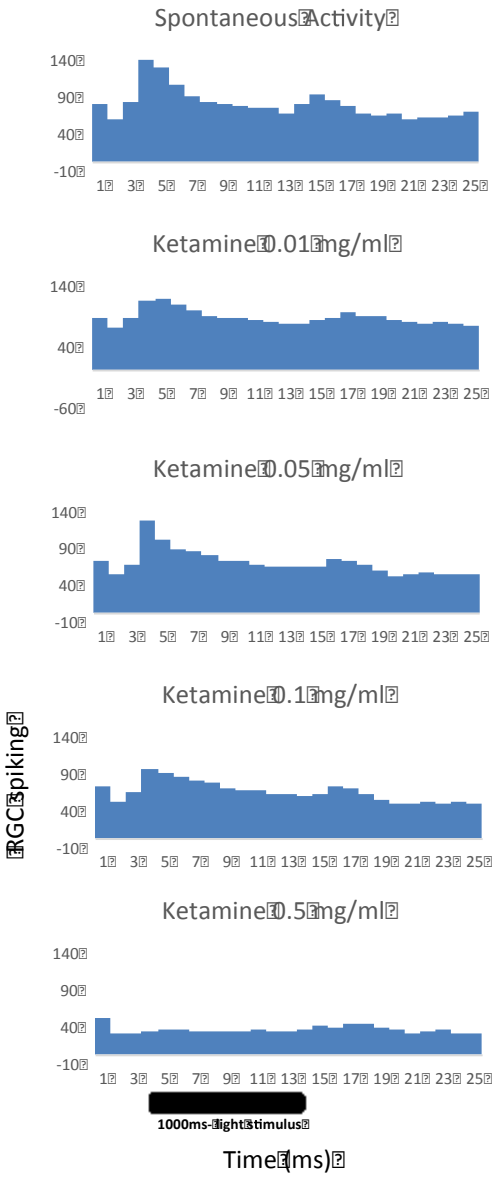

Figure 8.2. Peristimulus time histogram of average RGC spiking activity (frequency) over time (ms) at multiple concentrations of ketamine.

Averaged RGC spiking prior to normalization; black bar indicating 1000ms of light stimulus onset beginning at 300ms.

Table 2: Measures of central tendency and variation for overall ketamine experiments at each concentration. RatioKtotal= ratio of total retinal preparation spiking activity for each ketamine concentration (mg/ml) compared to baseline spiking activity (before addition of Ketamine).

RatioKtotal	Mean	Mean log	STDEV	STDEV log	Total Cell Count	SEM
Ket [0.01]	1.584	-0.009	1.904	0.486	82	0.210
Ket [0.05]	1.971	0.120	2.625	0.344	123	0.237
Ket [0.1]	1.300	0.005	0.986	0.320	123	0.089
Ket [0.5]	0.881	-0.581	2.492	0.667	82	0.275

The main effect of ketamine concentration on ganglion cell spiking was analyzed by using the log conversion of cell spiking (ratio of cell spiking of drug concentration to baseline), for normalization, for each concentration. A one-way MANOVA was performed for Drug effect.

A one-way MANOVA revealed a significant multivariate main effect for Drug Concentration, Wilks' λ=0.723, F (12, 995.094)=10.825, p<0.000, partial eta squared=0.103. Power to detect the effect was 1.0. Thus the hypothesis that drug concentration has an effect is confirmed.

Given the significance of the overall test, the univariate main effects were examined. Significant univariate main effects for Drug Concentration were obtained for RatioKctl (pre-stimulus period) F (3, 3.447)= 18.011, p<0.000, partial eta squared=0.125, power =1.0; RatioKctlON (during the ON stimulus) F(3, 9.825)= 40.790, p<0.000, partial eta squared=0.244, power= 1.0; RatioKctlOFF (during the OFF stimulus) F(3, 6.320)=24.098, p<0.000, partial eta squared=0.160, power = 1.0; and RatioKctlALL (total elicited over 1300msec) F(3, 6.523)=37.063, p<0.000, partial eta squared=0.227, power=1.0.

When analyzing the effect on a global scale for all ganglion cell types there was an increase in ratio of the total number of spikes per unit (~1.5x) compared to

baseline spiking at the lowest concentration of Ketamine (0.01mg/ml). Increasing the concentration to (0.05 mg/ml) resulted in a higher ratio of ketamine/baseline (~2x). At the highest concentration (0.5 mg/ml) there was a slight decrease in ratio of the total number of spikes compared to baseline values (~0.8x) (Figure 9). Significant differences in mean spiking ratio (ketamine concentration compared to baseline) were observed between all concentrations (0.01mg/ml; 0.05mg/ml; 0.1mg/ml) compared to the highest concentration (0.1mg/ml); p=0.000. Additionally, one-sample t-tests revealed significant differences in the mean spiking ratio (figure 9 [*]) for ketamine 0.05mg/ml and ketamine 0.1mg/ml, compared to the null hypothesis of a 1:1 no change ratio within the cells of those concentrations.

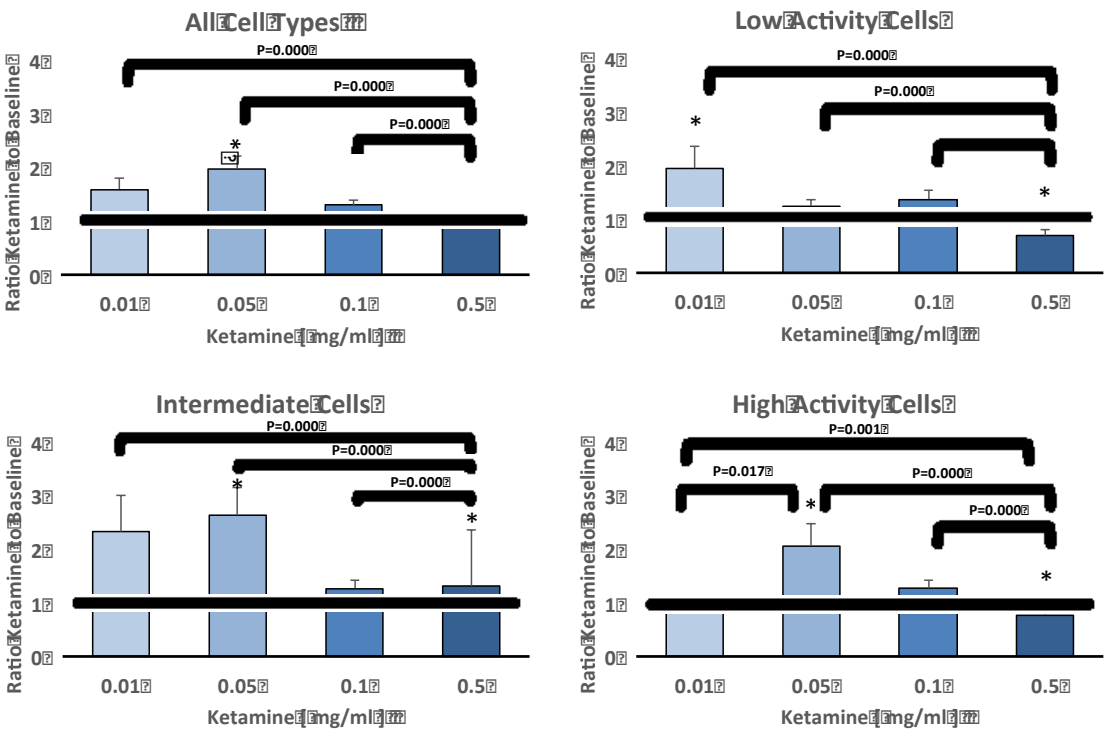

Figure 9. Mean ratio of ganglion cell spiking activity (total response) in ketamine concentrations compared to baseline spiking activity for all cell spiking types, low activity, intermediate activity and high activity cells. Whole data shown for illustration, log transformed data used for statistical analysis.

- *Significant MANOVA Pairwise Difference of Means denoted with black bars and p-values for "All Cell Types".*
- *Significant ANOVAs denoted with black bars and p-values for "Low, Intermediate and High Activity Cells". There was a significant difference amongst all lower concentrations of ketamine compared to the highest concentration for all cell types (top left), p=0.000; for low activity cells (top right), p=0.000; and for intermediate activity cells (bottom left), p=0.000. High activity cells had a significant difference for all compared to highest concentration (p=0.001, p=0.000) and also for ketamine 0.01mg/ml to ketamine 0.05mg/ml, p=0.017.*

- *Significant t-test indicated with asterisk (*). The mean difference in the population mean in All Cell Types for ketamine 0.05mg/ml is 0.11951, 95% CI [0.0580 to 0.1810], t (122) =3.848, p=0.000. The mean difference in the population mean in Low Activity cells for ketamine 0.01mg/ml is 0.18116, 95% CI [0.0556 to 0.3068], t(21)=3.0, p=0.007. The mean difference in the population mean in Low Activity cells for ketamine 0.5mg/ml is -0.35951, 95% CI [-0.5750, -0.1440], t(21)=-3.470, p=0.002. The mean difference in the population mean in Intermediate Activity cells for ketamine 0.05mg/ml is 0.22729, 95% CI [0.825, 0.3720], t(30)=3.207, p=0.003. The mean difference in the population mean in Intermediate Activity cells for ketamine 0.5mg/ml is -0.84967, 95% CI [-1.2105, -0.4889], t(19)=-4.929, p=0.000. The mean difference in the population mean in High Activity cells for ketamine 0.05mg/ml is -0.11832, 95% CI [0.0277, 0.2089], t(56)=2.617, p=0.011. The mean difference in the population mean in High Activity cells for ketamine 0.5mg/ml is -0.56821, 95% CI [-0.7840, -0.3525], t(38)=-5.331, p=0.000.*

6.1.2 GLOBAL EFFECT ON CELL TYPE

The effect of ketamine on cell type was analyzed by using the log conversion of cell type spiking (ratio of cell type spiking of drug concentration to baseline), for normalization, for each concentration. A one-way MANOVA was performed for Cell Type.

A one-way MANOVA revealed no significant multivariate main effect for Cell Type, Wilks' $\lambda = 0.968$, $F(8, 752) = 1.564$, $p<0.132$, partial eta squared =0.016. Power to detect the effect was 0.702. Thus the hypothesis that application of ketamine on the retinal preparation differentially affects the RGCs according to their degree of tonicity is not confirmed.

A one-way ANOVA revealed a significant effect of drug concentration on low activity cell types, F[3, 108)=10.402, p=0.000]; for intermediate cell types, F[3,

98)=21.945, p=0.000]; and for high activity cell types, F[3, 189)=18.908, p=0.000](Figure 9).

The behavior of the individual cells varies based on cell type (Figure 10). Low activity cells behaved slightly differently. At the lowest concentration the activity was increased and continued to increase at higher drug concentrations, with a reduction in activity seen at 0.5 mg/ml. Cells with an intermediate style of spiking behaved very similar to that of the global experiment. Higher activity cells showed less of an increase at the lowest dose and a decrease in activity at the highest drug concentration (0.5 mg/ml).

Despite the significant global effects observed, not all cells behaved in the same way. For instance at the lowest concentration of ketamine, 0.01mg/ml, lower activity cells had a 9% reduction in firing compared to higher activity cells that showed a 42% reduction (Table 3). Lower activity cells show a greater reduction (26%) at an increased concentration of ketamine (0.05mg/ml) despite other lower activity cells in the population showing a general increase (46%). At the higher concentrations of ketamine (0.01mg/ml and 0.5mg/ml) the percentage of cells remaining in a similar state of firing was less frequent as was the tendency to show more of a reduction in behavior compared to an increase for all three types of cells.

Table 3. Percent change in cell behavior in function of parts of the responses and cell types.

Increased (%)	52	68	55	43
Reduced (%)	32	9	35	42
Similar (%)	16	23	10	15
Increased (%)	49	46	58	46
Reduced (%)	26	26	16	31
Similar (%)	25	28	26	23
Increased (%)	47	49	52	44
Reduced (%)	42	40	42	44
Similar (%)	11	11	6	12
Increased (%)	18	23	52	20
Reduced (%)	77	59	42	80
Similar (%)	5	18	6	0

Ketamine administration resulted in an increase of spontaneous firing of cells at all dosages compared to baseline activity (Figure 10). When dividing cells into low, intermediate and high activity classifications there were differences when compared to overall responses. The spontaneous firing of intermediate activity type cells increased more at higher concentrations (ketamine 0.1 mg/ml and 0.5 mg/ml) and reduced at lower concentrations. Intermediate type cells show reduced firing rates compared to baseline at all drug concentrations, with the greatest reduction at the highest concentration (0.05 mg/ml). Higher activity cell types reduced activity at the lowest (0.01 mg/ml) and highest (0.5 mg/ml) concentrations of ketamine, but showed an increase in activity with concentrations in mid-range (0.05 mg/ml and 0.1 mg/ml).

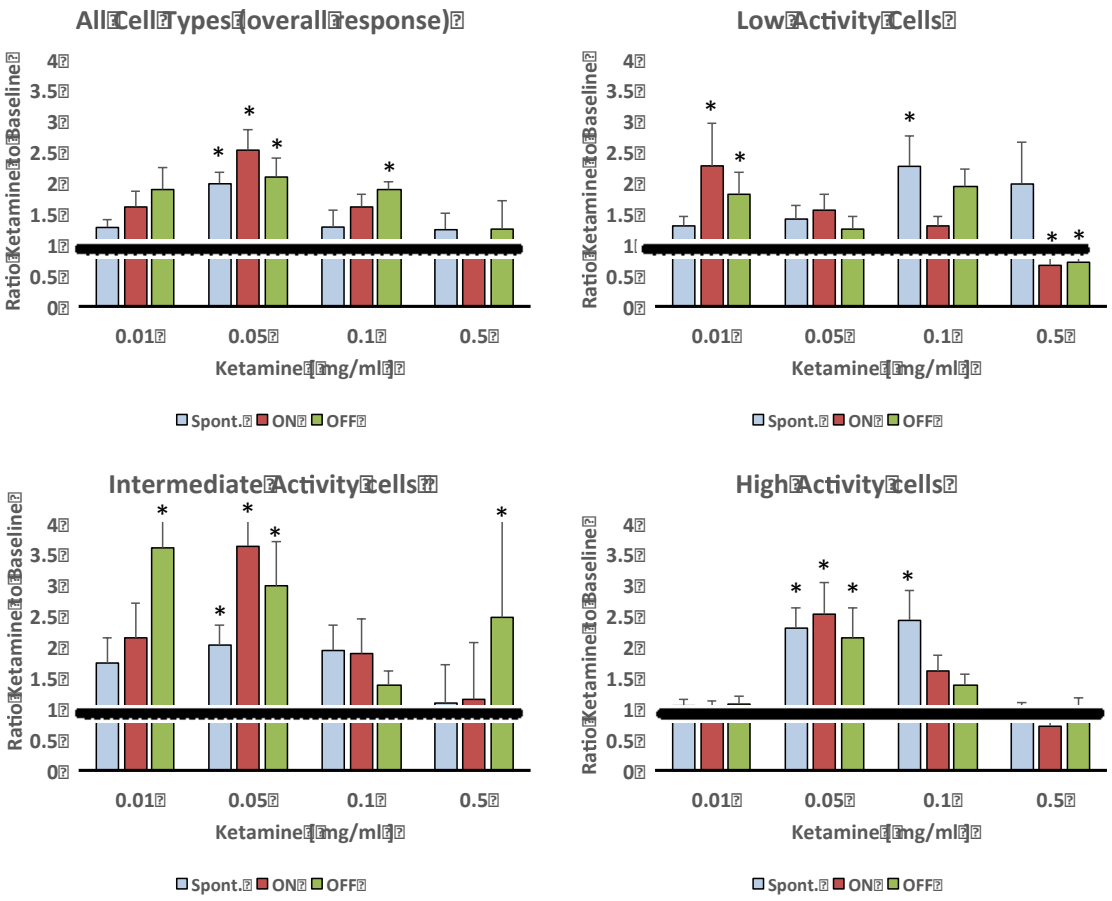

Figure 10. Ratio of ganglion cell spiking of spontaneous activity, ON response and OFF response in ketamine concentrations compared to baseline spiking for all cells, low activity, intermediate activity and high activity cells. Whole data shown for illustration, log transformed data used for statistical analysis. Significant t-test indicated with asterisk (*).

- *The mean difference in the population mean in All Cell Types OFF response for ketamine 0.05mg/ml is 0.10512, 95% CI [0.0338 to 0.1765], than the normal ratio of 1.0 (0 log transformed), t (121) =2.917, p=0.004. The mean difference in the population mean for All Cell Types ON responses for ketamine 0.05mg/ml is 0.16368, 95% CI [0.0906 to 0.2367],t (121) =4.435, p=0.000. The mean difference in the population mean for All Cell Types spontaneous activity for*

ketamine 0.05mg/ml is 0.15841, 95% CI [0.0993 to 0.2175],t (120) =5.310, p=0.000.

- *The mean difference in the population mean in Low Activity cells ON responses for ketamine 0.01mg/ml is 0.16706, 95% CI [0.0048 to 0.3294], t(21)=2.140, p=0.044. The mean difference in the population mean in Low Activity cells OFF responses for ketamine 0.01mg/ml is 0.17418, 95% CI [0.0400 to 0.3083], t(20)=2.708, p=0.014. The mean difference in the population mean in Low Activity cells spontaneous activity for ketamine 0.1mg/ml is 0.16891, 95% CI [0.0179 to 0.3199], t(31)=2.281, p=0.030. The mean difference in the population mean in Low Activity cells ON responses for ketamine 0.5 mg/ml is -0.46304, 95% CI [-0.7335 to -0.1926], t(21)=-3.561, p=0.002. The mean difference in the population mean in Low Activity cells OFF responses for ketamine 0.5 mg/ml is -0.42619, 95% CI [-0.7421 to -0.1103], t(19)=-2.824, p=0.011.*
- *The mean difference in the population mean in Intermediate Activity cells OFF responses for ketamine 0.01mg/ml is 0.16706, 95% CI [0.0048 to 0.3294], t(21)=2.140, p=0.000. The mean difference in the population mean in Intermediate Activity cells spontaneous activity for ketamine 0.05mg/ml is 0.18855, 95% CI [0.0737 to 0.3034], t(30)=3.354, p=0.002. The mean difference in the population mean in Intermediate Activity cells ON responses for ketamine 0.05mg/ml is 0.26672, 95% CI [0.0906 to 0.4429], t(30)=3.092, p=0.004. The mean difference in the population mean in Intermediate Activity cells OFF responses for ketamine 0.05mg/ml is 0.23645, 95% CI [0.0782 to 0.3947], t(30)=3.051, p=0.005. The mean difference in the population mean in Intermediate Activity cells OFF responses for ketamine 0.5mg/ml is -0.66889, 95% CI [-1.1137 to -0.2241], t(18)=-3.159, p=0.005.*
- *The mean difference in the population mean in High Activity cells spontaneous activity for ketamine 0.05mg/ml is 0.19647, 95% CI [0.1012 to 0.2918], t(56)=4.130, p=0.000. The mean difference in the population mean in High Activity cells ON responses for ketamine 0.05mg/ml is 0.16917, 95% CI [0.0646 to 0.2738], t(55)=3.241, p=0.002. The mean difference in the population mean in*

High Activity cells OFF responses for ketamine 0.05mg/ml is 0.09491, 95% CI [-0.0132 to 0.2030], t(56)=1.758, p=0.054. The mean difference in the population mean in High Activity cells spontaneous activity for ketamine 0.1mg/ml is 0.09953, 95% CI [-0.0292 to 0.2282], t(56)=1.549, p=0.013.

When broken down into cell types the sample size was not uniform across groups so the estimated marginal means were assessed (Figure 11). The estimated marginal mean is an unweighted mean, accounting for each mean in a population (cell type), compared across different sample sizes. Across all cell types the lowest marginal mean was seen in intermediate firing cells at the highest ketamine concentration 0.5mg/ml. Low activity cells, showed the least variation in marginal means across ketamine concentrations for each cell type. A moderate concentration of ketamine 0.01mg/ml showed the least effect on the marginal mean for low, intermediate and high activity cell firing across all cell types (Spontaneous firing, ON and OFF).

Additional qualitative looks at cell spiking shows sustain response properties of a cells responding to the light stimulus (Figure 12). The ratio of cell spiking within the first 300ms and last 400ms for ON- and OFF- type responses was compared. The higher the ratio the more prompt/ brisk the response was. With increased ketamine concentration ON cells show a more sluggish response compared to lower concentrations. Response remained at a more consistent ratio at every concentration for OFF cells.

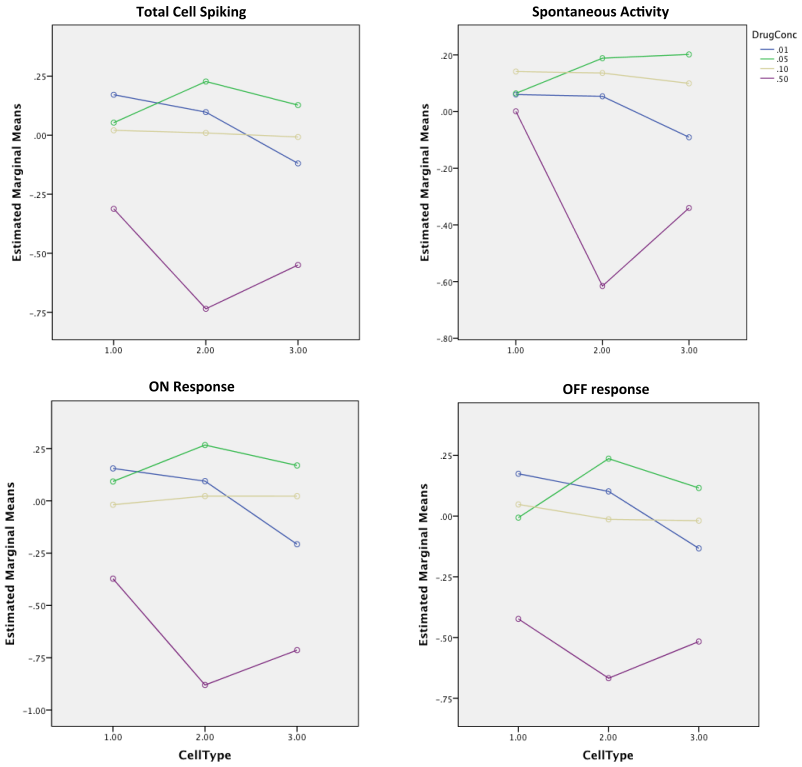

Figure 11. Estimated marginal means for the ratio of cell spiking at different ketamine concentrations for the overall experiment and for spontaneous cell spiking, ON cell spiking and OFF cell spiking.

Low activity cells (1.00), intermediate cells (2.00) and high activity cells (3.00) along x-axis; estimated marginal means y-axis. Drug concentration: ketamine 0.01mg/ml (blue), ketamine 0.05mg/ml (green), ketamine 0.1mg/ml (yellow) and ketamine 0.5mg/ml (purple).

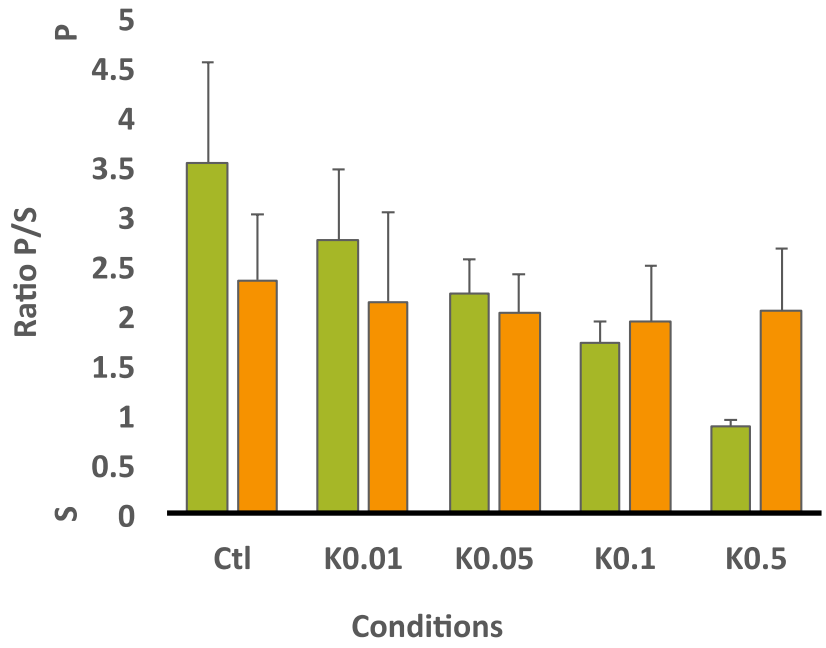

Figure 12. Ratio of early response (first 300ms) to later response (last 400ms) for ON (Green) and OFF (Orange) responses. Index of briskness of a response: S=Sluggish; P=Prompt. Ctl=baseline spontaneous activity; k=ketamine concentration (mg/ml).

6.2 XYLAZINE

6.2.1 GLOBAL EFFECT ON SPIKING RATIO

Peristimulus time histograms, sum of all cell activity recorded on the MEA, were created by averaging spiking activity across the duration of the light stimulus. These values were then normalized to allow for inter cell variations. The histograms show the spontaneous activity prior to the onset of the stimulus, the responses during the flash and cell responses directly after the flash. A long duration flash was used to separate ON from OFF components. The amount of cell spiking did not

appear to show a significant reduction; however there seemed to be a shift in when the cells were spiking (Figure 13) as the concentration of xylazine increased.

There was an increase in mean cell spiking ratio of all ganglion cell responses (including spontaneous activity, ON and OFF response) in the experiment compared to baseline for xylazine concentrations 0.0004mg/ml and 0.04mg/ml (Table 4). At the xylazine concentration of 0.004mg/ml the ratio appeared unchanged whereas for the highest concentration of xylazine (0.4mg/ml) the ratio was reduced.

The main effect of xylazine concentration on ganglion cell spiking was analyzed by using the log conversion of cell spiking (ratio of cell spiking of drug concentration to baseline), for normalization, for each concentration. A one-way MANOVA was performed for Drug effect.

A one-way MANOVA revealed a significant multivariate main effect for Drug Concentration, Wilks' λ=0.671, F (12, 791.371)=10.724, p<0.000, partial eta squared=0.124. Power to detect the effect was 1.0. Thus the hypothesis that drug concentration has an effect is confirmed.

Given the significance of the overall test, the univariate main effects were examined. Significant univariate main effects for Drug Concentration were obtained for RatioXctlON F (3, 3.732)=27.334, p<0.000, partial eta squared=0.214, power =1.0; RatioXctlOFF F(3, 2.334)=15.484, p<0.000, partial eta squared=0.133, power=1.0; RatioXctl F(3, 3.200)=14.394, p<0.000, partial eta squared =0.125, power=1.0; RatioXctlALL F(3, 3.227)=35.019, p<0.000, partial eta squared =0.258, power=1.0.

Significant mean differences in RatioXctlALL were obtained between Xylazine 0.0004mg/ml (M=0.073) and 0.4mg/ml (M=-0.492); between 0.004mg/ml (M=-0.043) and 0.04mg/ml (M=0.154); between 0.004mg/ml (M=-0.043) and 0.4mg/ml (M=-0.492); between 0.04mg/ml (M=0.154) and 0.4mg/ml (M=-0.492).

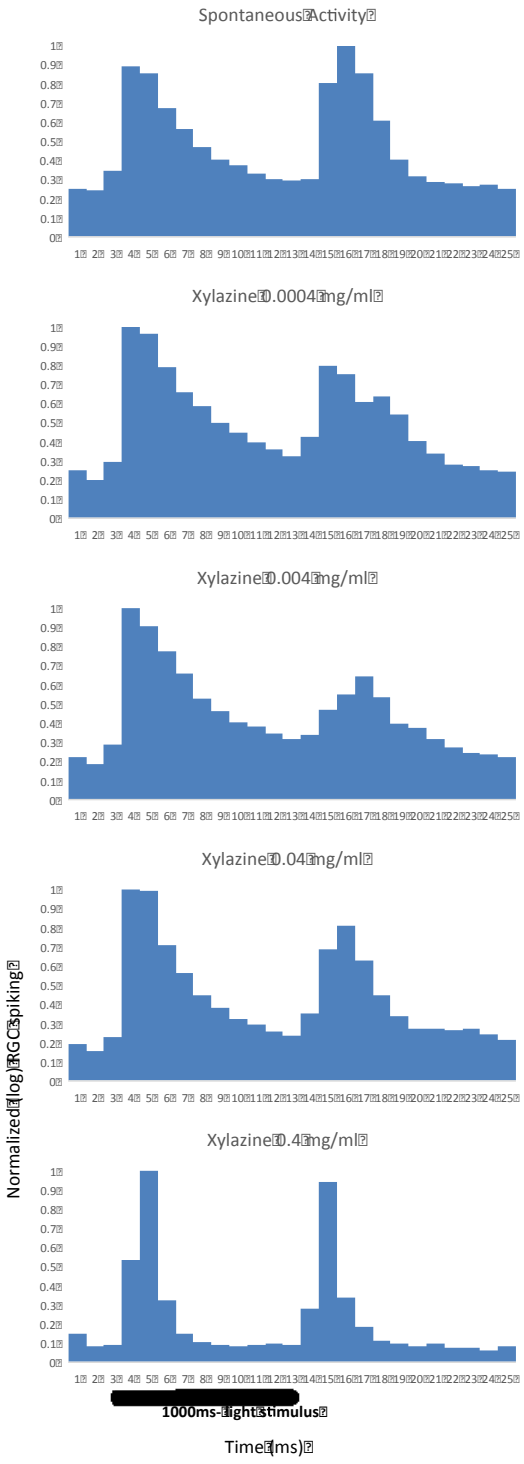

Figure 13.1. Peristimulus time histogram of average RGC spiking activity (frequency) over time (ms) at multiple concentrations of xylazine.

Normalized (log transformed) data; black bar indicating 1000ms of light stimulus onset beginning at 300ms.

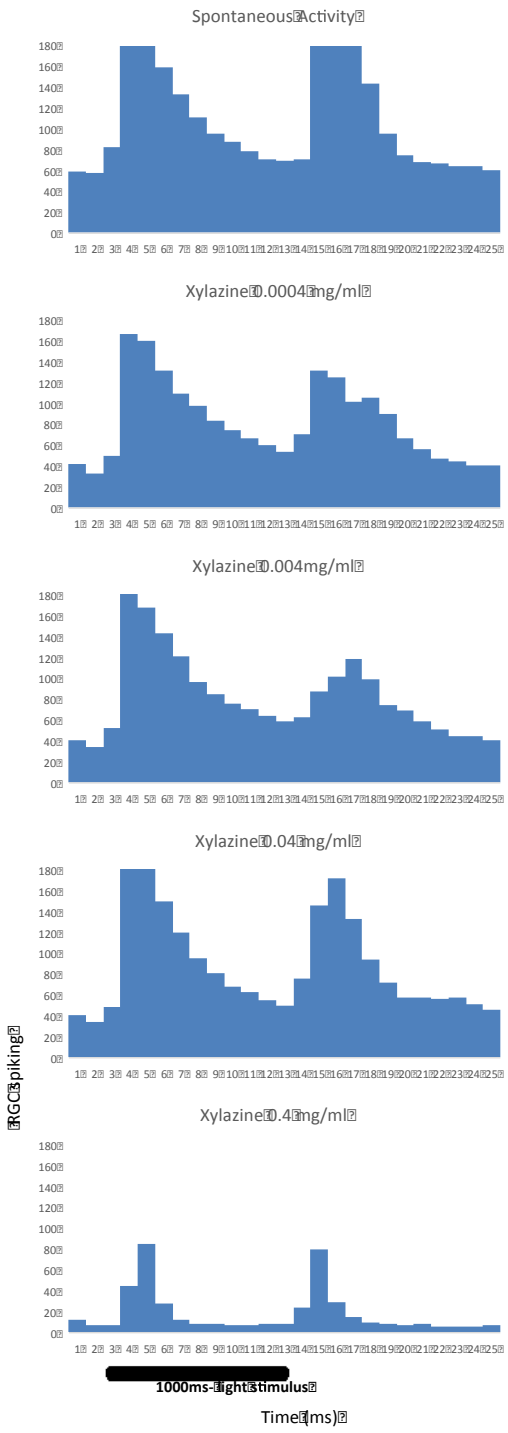

Figure 13.2. Peristimulus time histogram of average RGC spiking activity (frequency) over time (ms) at multiple concentrations of xylazine.

Averaged RGC spiking prior to normalization; black bar indicating 1000ms of light stimulus onset beginning at 300ms.

Table 4: Measures of central tendency and variation for overall xylazine experiments at each concentration.

RatioXtotal	Mean	Mean log	STDEV	STDEV log	Total Cell Count	SEM
Xyl [0.0004]	1.460	-0.049	2.676	0.409	106	0.260
Xyl [0.004]	0.996	-0.057	1.049	0.177	106	0.102
Xyl [0.04]	1.709	0.145	1.507	0.261	103	0.149
Xyl [0.4]	0.377	-0.732	0.446	0.595	102	0.044

When analyzing the effect on a global scale for all ganglion cell types there was an increase in ratio of the total number of spikes per unit (~1.5x) compared to baseline spiking at the lowest concentration of xylazine (0.0004mg/ml). Increasing the concentration to (0.004 mg/ml) resulted in no change in ratio of xyalzine/baseline (~1x). At the highest concentration (0.4 mg/ml) there was a decrease in ratio of the total number of spikes compared to baseline values (~0.4x) (Figure 14). Significant differences in mean spiking ratio (Xylazine concentration compared to baseline) were observed between all concentrations (0.0004mg/ml; 0.004mg/ml; 0.04mg/ml) compared to the highest concentration (0.4mg/ml); p=0.000. Additionally, one-sample t-tests revealed significant differences in the mean spiking ratio (figure 14 [*]) for xylazine 0.04mg/ml and xylazine 0.4mg/ml, compared to the null hypothesis of a 1:1 no change ratio within the cells of those concentrations.

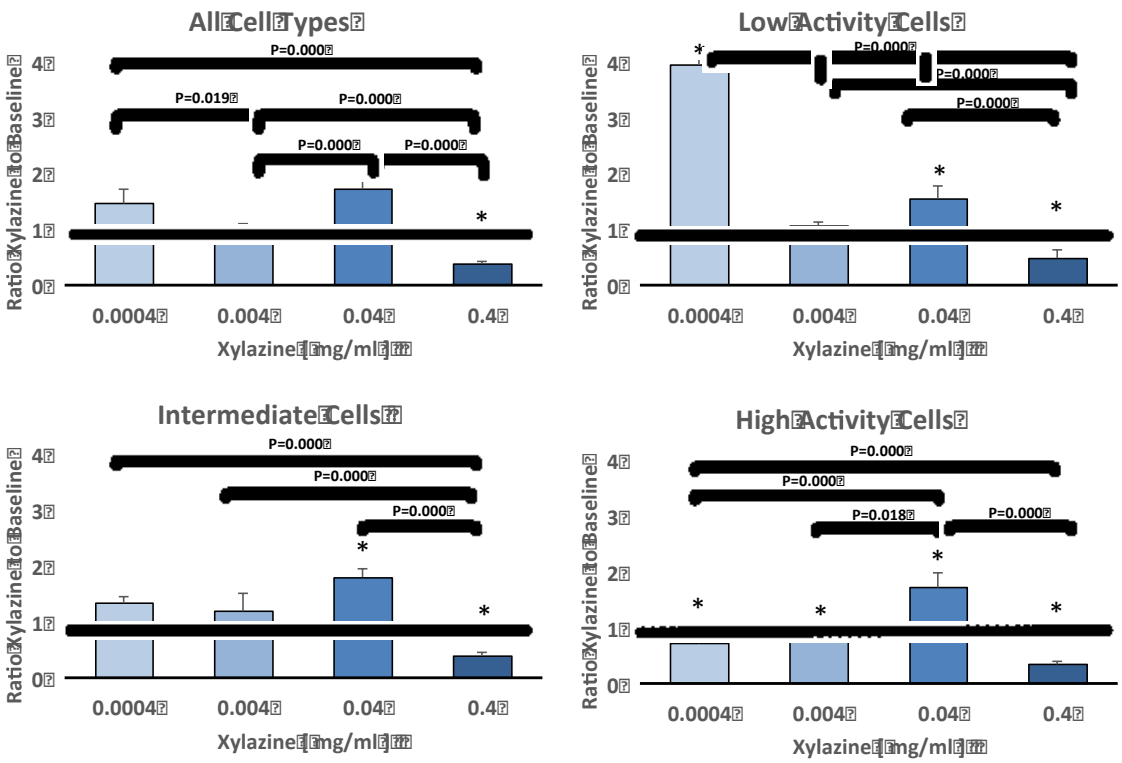

Figure 14. Mean ratio of ganglion cell spiking activity (total response) in xylazine concentrations compared to baseline spiking activity for all cell spiking types, low activity, intermediate activity and high activity cells. Whole data shown for illustration, log transformed data used for statistical analysis.

- *Significant MANOVA Pairwise Difference of Means denoted with black bars and p-values for "All Cell Types".*
- *Significant ANOVAs denoted with black bars and p-values for "Low, Intermediate and High Activity Cells". There was a significant difference amongst all lower concentrations of xylazine compared to the highest concentration for all cell types (top left), p=0.000; There was a significant difference in xylazine 0.0004mg/ml and 0.004mg/ml, p=0.019. Between 0.004mg/ml and 0.04mg/ml, p=0.000. There was a significant difference for low activity cells across all concentrations (top right), p=0.000; there was also a difference between xylazine 0.0004mg/ml and all higher concentrations, p=0.000. There was a significant difference between all lower concentrations*

compared to the highest concentration 0.4mg/ml for intermediate activity cells (bottom left), p=0.000. High activity cells had a significant difference for xylazine 0.0004mg/ml and 0.04mg/ml, p=0.000; between 0.0004mg/ml and 0.4mg/ml, p=0.000; between 0.004mg/ml and 0.04mg/ml, p=0.018; between 0.04mg/ml an d0.4mg/ml, p=0.000

- *Significant t-test indicated with asterisk (*). The mean difference in the population mean in All Cell Types for xylazine 0.04mg/ml is -0.05728, 95% CI [-0.0914 to -0.0232], t (105) =-3.334, p=0.001. The mean difference in the population mean for xylazine 0.4mg/ml is -0.73194, 95% CI [-0.8488 to -0.6151], t (101) =-12.430, p=0.000. The mean difference in the population mean in Low Activity cells for ketamine 0.01mg/ml is 0.18116, 95% CI [0.0556 to 0.3068], t(21)=3.0, p=0.007. The mean difference in the population mean in Low Activity cells for xylazine 0.0004mg/ml is 0.35347, 95% CI 0.1540, 0.5529], t(17)=3.739, p=0.002.*

  The mean difference in the population mean in Low Activity cells for xylazine 0.04mg/ml is 0.13214, 95% CI [0.0174, 0.2469], t(15)=2.455, p=0.027. The mean difference in the population mean in Low Activity cells for xylazine 0.4mg/ml is -0.72960, 95% CI [-1.1208, -0.3384], t(15)=--3.976, p=0.001. The mean difference in the population mean in Intermediate Activity cells for xylazine 0.04mg/ml is 0.18493, 95% CI [0.0971, 0.2728], t(33)=4.283, p=0.000. The mean difference in the population mean in Intermediate Activity cells for xylazine 0.4mg/ml is -0.79319, 95% CI [-1.0411, -0.5453], t(32)=-6.517, p=0.000. The mean difference in the population mean in High Activity cells for xylazine 0.0004mg/ml is -0.24821, 95% CI [-0.3468, -0.1496], t(53)=-5.050, p=0.000. The mean difference in the population mean in High Activity cells for xylazine 0.004mg/ml is -0.08630, 95% CI [-0.1212, -0.0514], t(53)=-4.957, p=0.000. The mean difference in the population mean in High Activity cells for xylazine 0.04mg/ml is 0.12233, 95% CI [0.0453, 0.1993], t(52)=3.189, p=0.002. The mean difference in the population mean in High Activity cells for xylazine 0.4mg/ml is -0.73576, 95% CI [-0.8804, -0.5911], t(54)=-10.195, p=0.000.

6.2.2 GLOBAL EFFECT ON CELL TYPE

The effect of xylazine on cell type was analyzed by using the log conversion of cell type spiking (ratio of cell type spiking of drug concentration to baseline), for normalization, for each concentration. A one-way MANOVA was performed for Cell Type.

A one-way MANOVA revealed a significant multivariate main effect for Cell Type, Wilks' $\lambda = 0.910$, $F(8, 598) = 3.592$, $p<0.000$, partial eta squared $=0.046$. Power to detect the effect was 0.984. Thus the hypothesis that application of xylazine on the retinal preparation differentially affects the RGCs according to their degree of tonicity is confirmed.

A one-way ANOVA revealed a significant effect of drug concentration on low activity cell types, $F[3, 64)=19.615$, $p=0.000]$; for intermediate cell types, $F[3, 131)=38.024$, $p=0.000]$; and for high activity cell types, $F[3, 212)=56.304$, $p=0.000]$(Figure 14).

There was a significant difference in the ratio of ganglion cell spiking activity with the administration of xylazine compared to baseline for the entire preparation among low activity cells and intermediate activity cells, $p=0.003$ and among low activity cells and high activity cells, $p=0.000$.

Given the significance of the overall test, the univariate main effects were examined (Figure 14). Significant univariate main effects for Cell Type were obtained for RatioXcltON $(2, 0.776)= 5.683$, $p<0.004$, partial eta square= 0.036, power= 0.861; RatioXctlOFF $(2, 1.223)= 8.113$, $p<0.000$, partial eta square= 0.051, power=0.957; RatioXctlALL $(2, 0.888)=10.271$, $p<0.000$, partial eta square=0.064, power=0.987 (Figure 14).

The behavior of the individual cells varies based on cell type (Table 5). Low activity cells behaved slightly differently. At the lowest concentration (0.0004mg/ml) the activity was increased for low activity and intermediate cells whereas high activity cells showed more of the preparation shifting to reduced firing ratios. With xylazine 0.004mg/ml most cells remained within a similar firing state, whereas with an additional increase to 0.04mg/ml the firing rate shifted in

intermediate and high activity cells to show an increase in activity. At the highest concentration of xylazine we observed a decline in cell behavior in low and high activity cells but an increase in intermediate cell activity.

Significant mean differences in RatioXctlON were obtained between low activity cell types (type 1) (M=0.050) and intermediate cell types (type 2) (M=-0.167). Significant mean differences in RatioXctlON were obtained between cell types 1 (M=0.050) and high activity cell types (type 3) (M=-0.167). Significant mean differences in RatioXctlOFF were obtained between cell type 1 (M=0.048) and cell type 3 (M=-0.198). Significant mean differences in RatioXctlALL were obtained between cell type 1 (M=0.059) and cell type 2 (M=-0.113). Significant mean differences in RatioXctlALL were obtained between cell type 1 (M=0.059) and cell type 3 (M=-0.178).

Table 5. Percent change in cell behavior in function of parts of the responses and cell types.

Increased (%)	29	61	50	6
Reduced (%)	38	0	21	61
Similar (%)	33	39	29	33
Increased (%)	15	28	15	11
Reduced (%)	32	11	35	37
Similar (%)	53	61	50	52
Increased (%)	57	44	65	57
Reduced (%)	15	6	12	19
Similar (%)	28	50	23	24
Increased (%)	9	13	65	7
Reduced (%)	87	75	12	93
Similar (%)	4	14	23	0

At the highest dose of xylazine there was a decrease in spontaneous activity (Figure 15). When intermediate concentrations of xylazine (0.004 mg/ml and 0.04

mg/ml) were added the spontaneous activity of the cells increased compared to baseline. This behavior was consistent for intermediate and high activity cells, however at the lowest dosage, low activity cells showed an increase in spiking. Low activity and intermediate activity cells had an increase in ON responses to the lowest concentrations (0.0004 mg/ml) of xylazine. ON responses also showed an increase in spiking activity to xylazine 0.04mg/ml for all activity types, but also show a decrease to the highest dosage 0.4 mg/ml. OFF responses followed a similar trend but were less affected at the highest dosage (0.4 mg/ml) compared to spontaneous activity and ON cells.

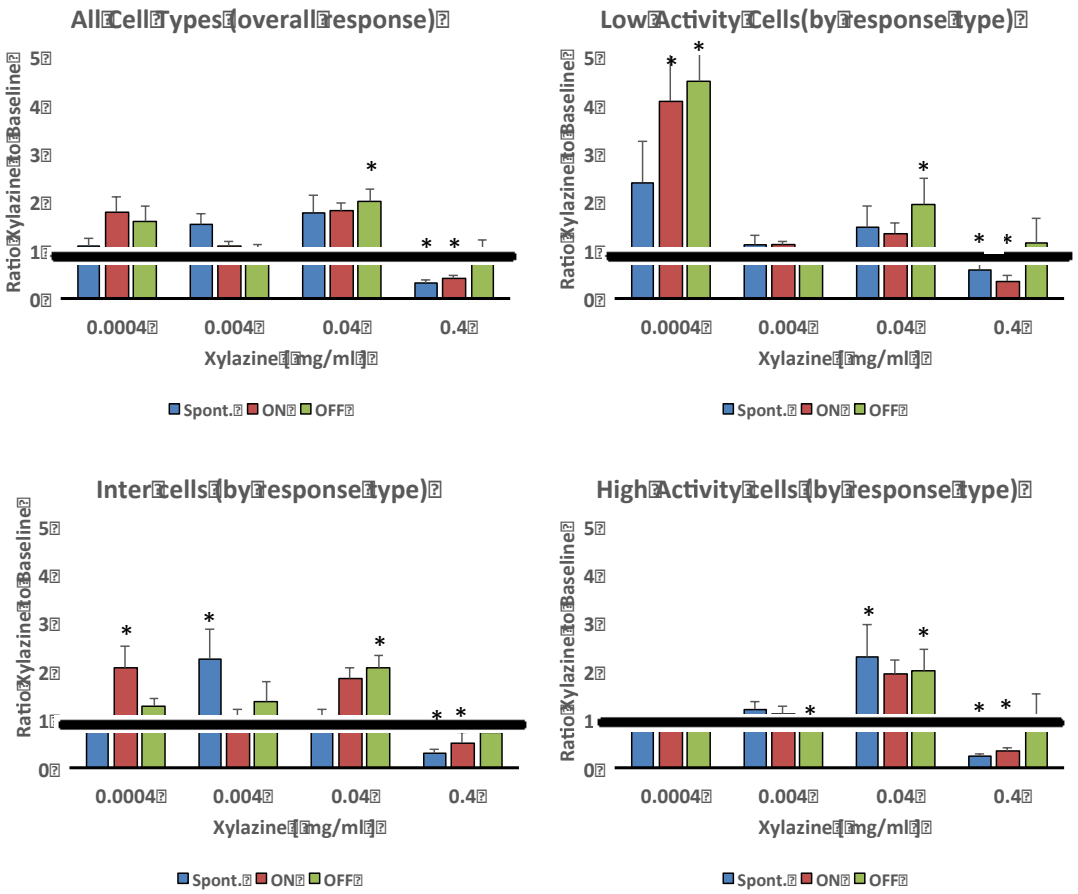

Figure 15. Ratio of ganglion cell spiking of spontaneous activity, ON response and OFF response in xylazine concentrations compared to baseline spiking for all cells, low activity, intermediate activity and high activity cells. Whole data shown for illustration, log transformed data used for statistical analysis. Significant t-test indicated with asterisk (*).

- *The mean difference in the population mean in All Cell Types OFF response for xylazine 0.04mg/ml is 0.13995, 95% CI [0.0687 to 0.2112], t (101) =3.894, p=0.000. The mean difference in the population mean for All Cell Types spontaneous activity for xylazine 0.4mg/ml is -0.74690, 95% CI [-0.8660 to -0.6278],t (94) =-12.447, p=0.000. The mean difference in the population mean for All Cell Types ON response for xylazine 0.4mg/ml is -0.51153, 95% CI [-0.6599 to -0.3631],t (86) =-6.852, p=0.000. The mean difference in the population mean for All Cell Types OFF response for xylazine 0.4mg/ml is -0.73194, 95% CI [-0.8488 to -0.6151],t (101) =-12.430, p=0.000.*

- *The mean difference in the population mean in Low Activity cells ON responses for xylazine 0.0004mg/ml is 0.32183, 95% CI [0.0785 to 0.5651], t(17)=2.791, p=0.013. The mean difference in the population mean in Low Activity cells OFF responses for xylazine 0.0004mg/ml is 0.35459, 95% CI [0.1302 to 0.5790], t(17)=3.335, p=0.004. The mean difference in the population mean in Low Activity cells ON response for xylazine 0.4mg/ml is -0.82090, 95% CI [-1.1777to -0.4641], t(15)=-4.905, p=0.000.*
- *The mean difference in the population mean in Intermediate Activity cells ON responses for xylazine 0.0004mg/ml is 0.11048, 95% CI [-0.0331 to 0.2541], t(33)=1.565, p=0.013. The mean difference in the population mean in Intermediate Activity cells spontaneous activity for xylazine 0.004mg/ml is 0.14629, 95% CI [0.0105 to 0.2821], t(31)=2.197, p=0.036. The mean difference in the population mean in Intermediate Activity cells OFF responses for xylazine 0.04mg/ml is 0.19341, 95% CI [0.0642 to 0.3244], t(33)=3.039, p=0.005. The mean difference in the population mean in Intermediate Activity cells spontaneous activity for xylazine 0.4mg/ml is -0.643, 95% CI [-1.07 to -0.22], t(15)=-3.221, p=0.006. The mean difference in the population mean in Intermediate Activity cells ON responses for xylazine 0.4mg/ml is -0.72277, 95% CI [-0.9869 to -0.4587], t(26)=-5.625, p=0.000.*
- *The mean difference in the population mean in High Activity cells spontaneous activity for xylazine 0.004mg/ml is -0.13812, 95% CI [-0.1938 to 0.0825], t(51)=-4.981, p=0.000. The mean difference in the population mean in High Activity cells spontaneous activity for xylazine 0.04mg/ml is 0.10014, 95% CI [-0.0324 to 0.2327], t(45)=1.522, p=0.014. The mean difference in the population mean in High Activity cells OFF responses for xylazine 0.04mg/ml is 0.11355, 95% CI [0.0169 to 0.2102], t(51)=2.359, p=0.022. The mean difference in the population mean in High Activity cells spontaneous activity for xylazine 0.4mg/ml is -0.61693, 95% CI [-0.8390 to -0.3948], t(25)=-5.721, p=0.000. The mean difference in the population mean in High Activity cells ON response for*

xylazine 0.4mg/ml is -0.73666, 95% CI [-0.8811 to -0.5922], t(51)=-10.236, p=0.000.

When broken down into cell types the sample size was not uniform across groups so the estimated marginal means were assessed (Figure 16). As mentioned previously the estimated marginal mean is an unweighted mean, accounting for each mean in a population (cell type), compared across different sample sizes. At the lowest concentration of xylazine (0.0004mg/ml) the marginal mean was highest for low activity type cells amongst all sections of cell spiking (Spontaneous, ON and OFF). At intermediate concentrations (0.004mg/ml & 0.04mg/ml) the means of ON responses behaved similar to the entire retinal output measurement with no significant change amongst low, intermediate or high cell types.

Additional qualitative looks at cell spiking shows sustain response properties of a cell to respond to the light stimulus (Figure 17). The ratio of cell spiking within the first 300ms and last 400ms for ON- and OFF- type responses was compared. The higher the ratio the more prompt/ brisk the response was. At lower and intermediate concentrations of xylazine both the ON- and OFF- type responses showed a similar response ratio. However, at the highest concentration both ON- and OFF- responses became more prompt/brisk.

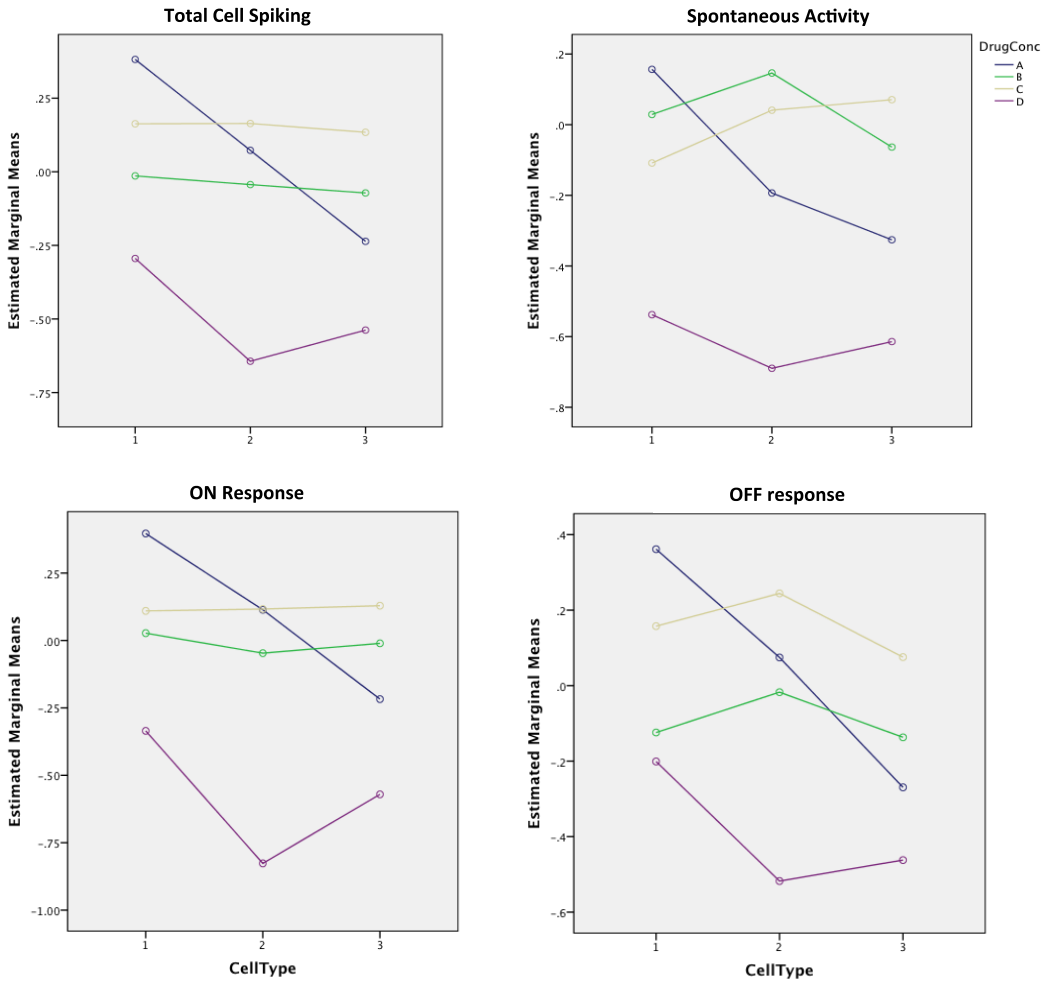

Figure 16. Estimated marginal means for the ratio of cell spiking at different xylazine concentrations for the overall experiment and for spontaneous cell spiking, ON cell spiking and OFF cell spiking.

Low activity cells (1.00), intermediate cells (2.00) and high activity cells (3.00) along x-axis; estimated marginal means y-axis. Drug concentration: xylazine 0.0004 mg/ml (blue), xylazine 0.004 mg/ml (green), xylazine 0.04 mg/ml (yellow) and xylazine 0.4 mg/ml (purple).

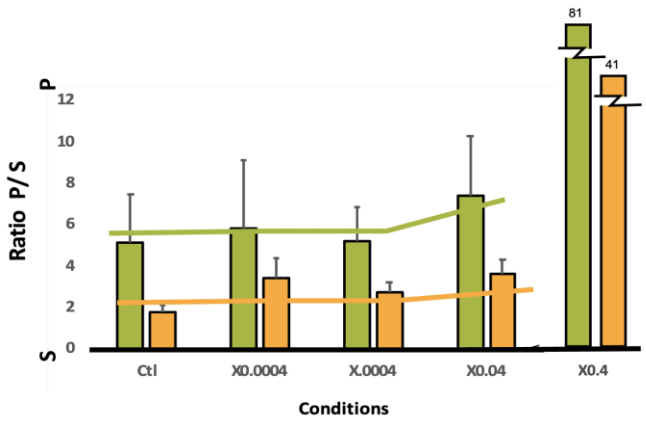

Figure 17. Ratio of early response (first 300ms) to later response (last 400ms) for ON (Green) and OFF (Orange) responses. Index of briskness of a response: S=Sluggish; P=Prompt. Ctl=baseline spontaneous activity; X=xylazine concentration (mg/ml).

6.3 COMBINED CONCENTRATION OF KETAMINE/XYLAZINE

6.3.1 GLOBAL EFFECT ON SPIKING RATIO

Peristimulus time histograms, sum of all cell activity recorded on the MEA, were created by averaging spiking activity across the duration of the light stimulus (Figure 18.2). These values were then normalized to allow for inter cell variations (Figure 18.1). The histograms show the spontaneous activity prior to the onset of the stimuli, the responses during the flash and cell responses directly after the flash. A long duration flash was used to separate ON from OFF components. The amount of cell spiking did not appear to show a significant reduction or shift in spiking activity after ketamine was administered, however there was a more noticeable change in spiking when xylazine was added in addition to a ketamine mixture.

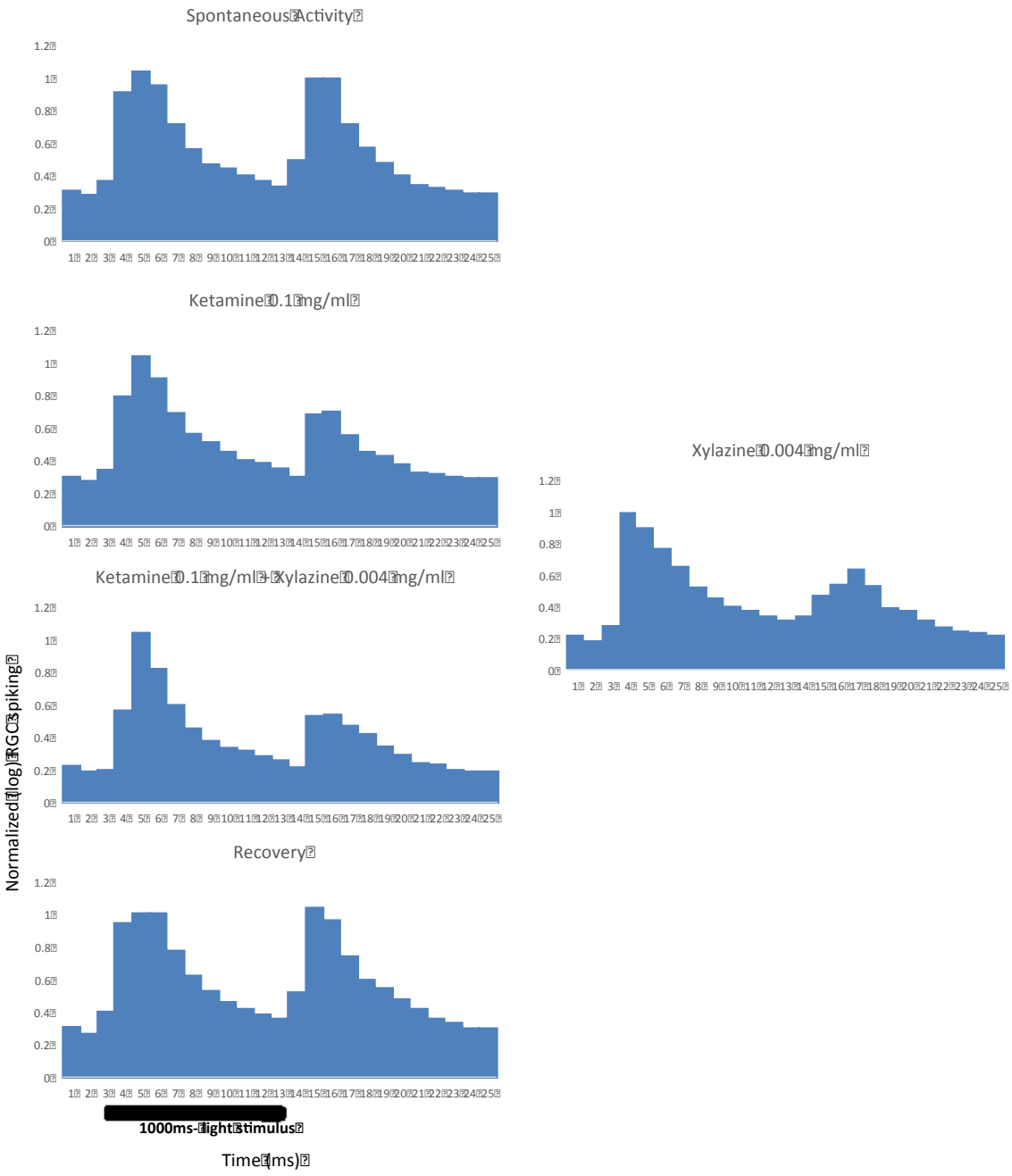

Figure 18.1: Peristimulus time histogram of average RGC spiking activity (normalized) over time (ms) at at ketamine 0.1mg/ml and ketamine 0.1mg/ml + xylazine 0.004mg/ml. xylazine 0.004mg/ml, from xylazine experiments, (right) for comparison. Black bar indicating 1000ms of light stimulus onset beginning at 300ms.

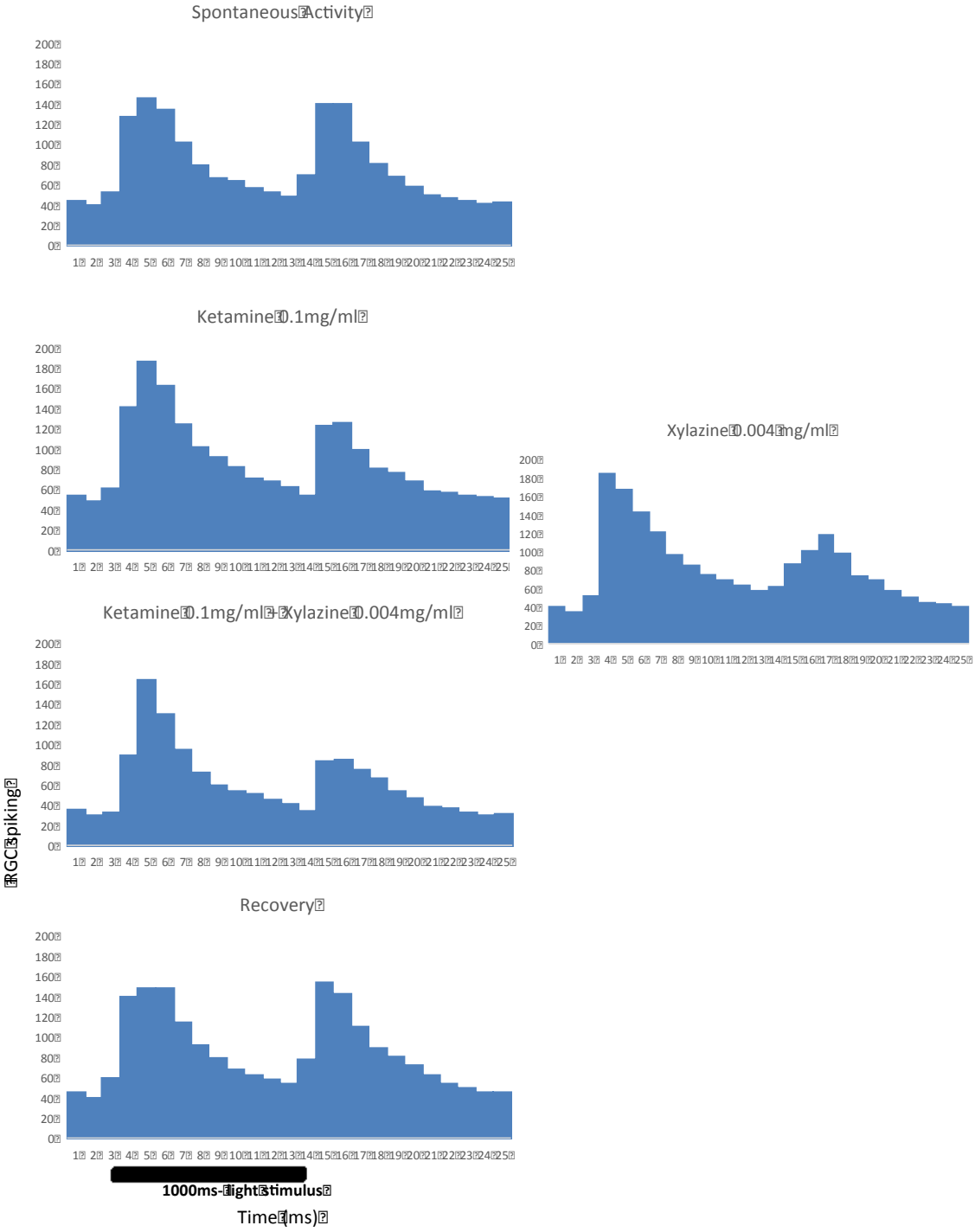

Figure: 18.2 Peristimulus time histogram of average RGC spiking activity (frequency) over time (ms) at ketamine 0.1mg/ml and ketamine 0.1mg/ml + xylazine 0.004mg/ml. xylazine 0.004mg/ml, from xylazine experiments, (right) for comparison. Black bar indicating 1000ms of light stimulus onset beginning at 300ms.

There was an increase in mean cell spiking ratio of all ganglion cell responses (Table 6) (including spontaneous activity, ON and OFF response) in the experiment compared to baseline for ketamine 0.01 mg/ml. When the combination of ketamine 0.01mg/ml + xylazine 0.004mg/ml were added there was an increase in mean cell spiking ratio of the total preparation compared to baseline.

Table 6. Measures of central tendency and variation for overall ketamine + xylazine experiments at each concentration.

Ratio total	Mean	Meanlog	STDEV	STDEV log	Total Cell Count
Ket [0.01]	1.36089	0.02649	1.34168	0.300888	164
Ket [0.01] + Xyl [0.004]	1.12387	-0.16293	1.44661	0.457178	164

The main effect of drug concentrations on ganglion cell spiking was analyzed by using the log conversion of cell spiking (ratio of cell spiking of drug concentration to baseline), for normalization, for each concentration. A one-way ANOVA was conducted to determine if the mean spiking ratio differed between ketamine 0.01mg/ml and ketamine 0.01mg/ml + xylazine 0.004mg/ml. A one-way ANOVA revealed there was no significant difference between groups ($F(1,326) = 2.367$, $p = 0.125$.

A one-way MANOVA was performed for Drug effect. A one-way MANOVA revealed a significant multivariate main effect for Drug Concentration, Wilks' $\lambda = 0.948$, $F(4, 272) = 3.760$, $p < 0.005$, partial eta squared=0.052. Power to detect the effect was 0.886. Thus the hypothesis that drug concentration has an effect is confirmed.

Given the significance of the overall test, the univariate main effects were examined. Significant univariate main effects for Drug Concentration were obtained

for OFF cell responses F (2, 275) =11.707, p<0.000, partial eta squared=0.078, power =0.994

For ketamine 0.01mg/ml the estimated margin means were highest for intermediate cell types for the global preparation, cells firing pre-stimulus (spontaneous activity), and for cells responding when the stimulus was on (ON response). When the combined drug (ketamine 0.01mg/ml + xylazine 0.004mg/ml) was added the estimated marginal means were highest for low activity cells for the global preparation and when broken down into pre-stimulus, ON stimulus and OFF stimulus cells (Figure 19).

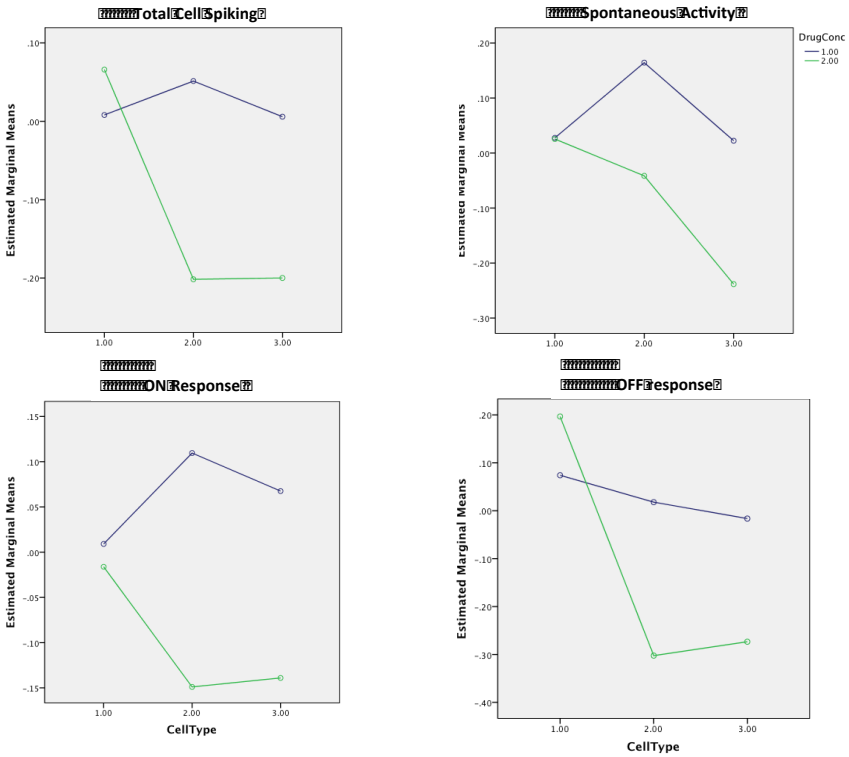

Figure 19: Estimated marginal means for the ratio of cell spiking at ketamine 0.1 mg/ml and ketamine 0.1 mg/ml + xylazine 0.004 mg/ml concentrations for the overall experiment and for spontaneous cell spiking, ON cell spiking and OFF cell spiking.

Low activity cells (1.00), intermediate cells (2.00) and high activity cells (3.00) along x-axis; estimated marginal means y-axis. Drug concentration: ketamine 0.1 mg/ml (blue), ketamine 0.01 + xylazine 0.004 mg/ml (green).

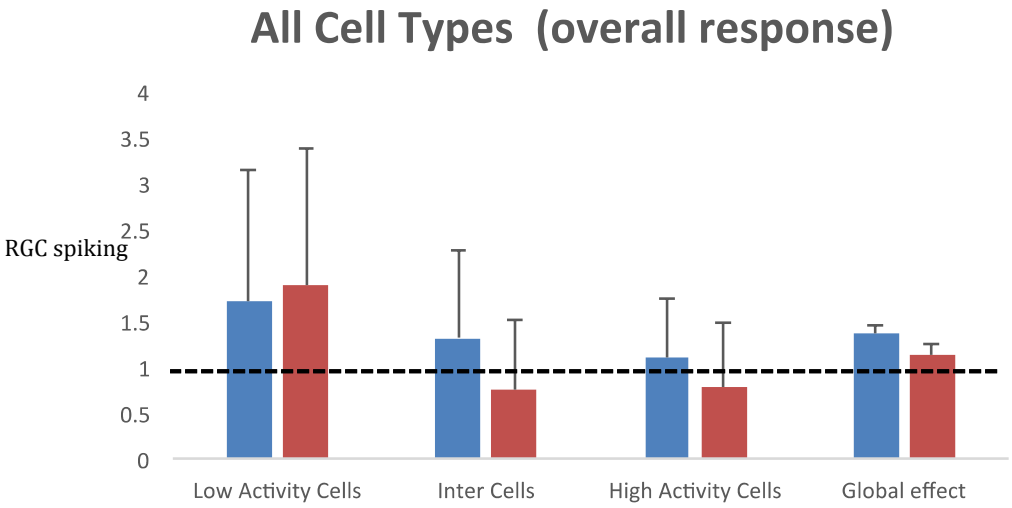

Figure 20: Ratio of ganglion cell spiking activity (frequency) in Ketamine 0.1mg/ml (blue) and ketamine 0.1mg/ml + xylazine 0.004mg/ml (red) concentrations compared to baseline spiking activity for all cell spiking types, low activity, intermediate activity and high activity cells. Dashed black line indicating a 1:1 ratio of no change.

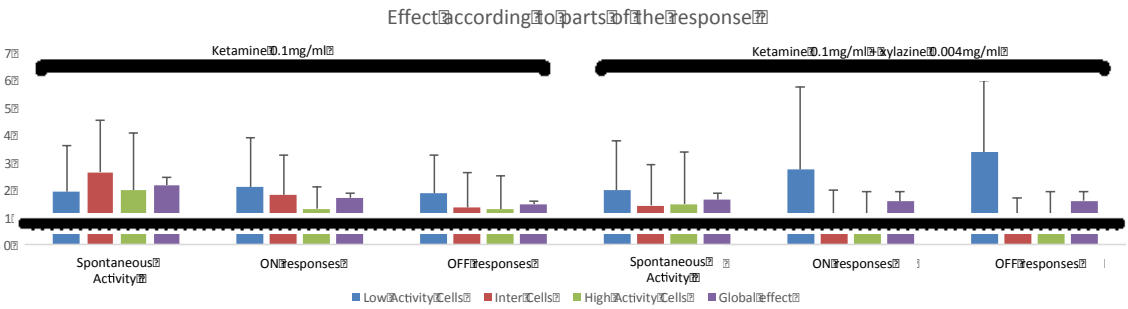

Figure 21: Ratio of ganglion cell spiking (frequency) in ketamine 0.01 mg/ml and ketamine 0.01mg/ml + xylazine 0.004mg/ml concentrations compared to baseline spiking for all cells, low activity, intermediate activity and high activity cells. Dashed black line indicating a 1:1 ratio of no change. Solid black line indicating ketamine 0.1 mg/ml versus ketamine 0.01mg/ml +xylazine 0.004mg/ml.

CHAPTER 7: DISCUSSION

7.1 IMPORTANT FINDINGS

During experimentation the mean retinal ganglion cell spiking (firing) rates had an increase compared to baseline mean RGC spiking with the addition of weaker concentrations of both ketamine and xylazine. The observed effect changed to a decline in mean RGC spiking when the concentrations were at the upper limits. Interestingly, when further examining the cells based on their response to light stimuli characteristic (i.e. Tonicity, ON- and OFF- cell responses) the mean RGC spiking was effected differently across groups.

We found a main effect of ketamine concentration on ganglion cell spiking with lower concentrations increasing the mean ratio of cell spiking rate compared to baseline values and the highest concentration of ketamine showing a decline in mean ganglion cell spiking compared to baseline. This observed effect appears to influence RGCs differently based on their tonicity, where lower activity (phasic) cells and intermediate activity cells showed higher ratios of increased firing at the lowest (subclinical) concentrations of ketamine while higher activity (tonic) cells showed increased spiking ratios at higher concentrations of ketamine. Ketamine is known to have inhibitory effects on NMDARs at the molecular level and may preferentially alter the function of NMDAs on interneurons. There are suggestions that both AMPA and NMDA receptors on retinal ganglion cells play complementary roles in synaptic transmission with AMPARs encoding spontaneous low-frequency presynaptic release and NMDARs encoding evoked, high frequency release (Manookin, 2010). Tonic neurons mediated by NMDA receptors have been hypothesized to be more vulnerable to excessive activation by glutamate, contributing to normal neuronal function and also to neuronal pathology (exocitotoxicity) (Povysheva & Johnson, 2012). Both ON and OFF cell responses showed increased cell spiking ratios at sub clinical concentrations of ketamine, however when the concentration reached non-physiological (likely toxic level) ON type cells showed more susceptibility compared to OFF responses. Manookin et al (2010) found the OFF cells within the retinas of

guinea pigs showed substantial NMDA responses that were mediated primarily by receptors composed of GluN2B subunits, whereas ON response expressed a relatively low level of NMDRAs.

Similarly, with our xylazine-treated cells we observed there was a main effect of concentration on ganglion cell spiking with an increase in spiking ratio compared to baseline spiking for lower concentrations and a decline in spiking to the highest concentration. Similar to ketamine we observed that lower activity (phasic) cells had the greatest increase in spiking at low dosages of xylazine and higher activity (tonic) cells showed more of an increase at higher drug concentrations, however all cells showed the decline in spiking at our highest dosage of xylazine. Pluteanu et al (2002) found α-adrenoreceptor stimulation of dorsal root ganglions in rats induced depolarization and increased excitability. Other selective α2-adrenoceptor agonists, such as Brimondine, have been shown to have neuroprotective qualities as it improves the survival rate of retinal ganglion cells after calibrated optic nerve injury in rats (Ahmed et al, 2001). There is increasing evidence that within different types of CNS injury, such as glutamate excitotoxicity and oxidative stress, different pathways of cell apoptosis are activated. Cell death within a hypertensive eye may occur due to excess glutamate, resulting in activation of NMDA receptors, cascading into increased uptake of Ca^{2+} and eventually cell death (Choi, 1988, Ahmed et al, 2001). Models of ischemic injury and trauma where cellular energy decreases, shifting the ionic balance, have been speculated to cause more depolarization of nerve membrane potential and a pathological release of glutamate. In this condition a α_2 -adrenoreceptor agonist could potentially cause a decrease in the release of glutamate from neurons (Donello et al, 2000, Ahmed et al, 2001).

When both drugs were co-administered we observed a shift in the mean ratio of ganglion cell spiking based on the cell's tonicity. Lower activity cells (phasic) cells maintained a higher mean spiking ratio, while intermediate and high activity (tonic) cells showed a decline in mean spiking activity.

7.2 TECHNICAL CONSIDERATIONS

The average number of cells obtained per retinal preparation; with reliable ganglion cell-spiking response to the light stimuli was 20.0 +/- 13.4. There were a total of 378 cells that maintained firing (119 exposed to ketamine concentrations, 102 exposed to xylazine concentrations, and 157 exposed to the combination of drugs) after excluding some retinal ganglion cells that showed irregular evoked firing patterns or no reliable evoked responses. Although many studies on MEA recordings do not expand on cell counts these findings appear similar to those obtained by Ryu et al (2009). The average number of retinal ganglion cells per patch was 46.75 +/- 4.39 with 11.5 +/- 4.03 per patch showing consistent evoked responses by stimulation. We used the recovery (post retinal washout with AMES solution) as the next experimental drug concentrations baseline recording. Due to some cells not maintaining a firing rate above background noise the control groups showed some variation among different drugs.

For this experiment we chose to use the multi-electrode array (MEA) to record our data set because of its ability to record multiple evoked-responses in parallel at different electrodes within one piece of retina. This technique allowed for reliable large scale screening of a targeted effect from the administered drug concentrations. Additional electrophysiology techniques in the literature, such as the patch clamp technique, provide high resolution recordings which are ideal in precise physiological and pharmacological investigations when trying to understanding mechanisms of action. The patch clamp technique has the ability to address effects on specific neurons, receptor systems or neurotransmitters; however is limited to recording from a single neuron down to single channel.

7.3 PLASMA CONCENTRATIONS

Concentrations of ketamine and xylazine for our MEA experimentation were determined by including both the low end of anticipated (sub-anesthetic) plasma concentrations and the high end (non-physiological higher levels) found in current

literature. (Tables 1,7). There were some limitations in the review as not all papers reported blood plasma concentrations of the drugs at various levels of anesthesia. Additionally fewer studies were available on plasma concentrations of xylazine in comparison to ketamine, especially in a guinea pig or rodent model. Another factor considered was different tissues in the body, especially within the CNS have been documented to hold higher concentrations of anesthetics compared to those measured in blood plasma. Tissues such as the brain/CNS have been documented to be up to five times higher in anesthetic concentrations (Stoelting, 1999). Ikeda et al (2010) observed the sum of protein-bound and unbound fractions of anesthetics found in the cerebral extracellular fluid and bound to brain parenchyma was approximately 2-3 times higher compared to plasma concentrations.

Table 7. Known blood plasma concentrations at sub-anesthetic and clinical anesthetic concentrations with experimental drug concentrations used for MEA experimentation.

	Plasma [] range	**Reference**	**Experimental [] range**
Ketamine	200- 10,000ng/ml	Clements & Nimmo (1981); Veilleux-Lemieux et al (2013)	10,000 -500,000ng/ml
Xylazine	150- 10,000ng/ml	Niedorf et al (2003); Veilleux-Lemieux et al (2013)	400- 400,000 ng/ml
Combined	10,000 ng/ml ketamine 1,000 ng/ml xylazine	Veilleux-Lemieux et al (2013)	10,000 ng/ml ketamine 4,000 ng/ml xylazine

Malinovsky et al (1996) examined the pharmacokinetics of Ketamine and Norketamine after nasal, rectal and i.v. administration in young children. They found the mean plasma concentration peaked at 496 ng/ml after nasal administration, and 632 ng/mlafter rectal administration. Yangaihara et al (2003) conducted another study in humans to assess plasma concentrations of low dose Ketamine where analgesic effects were desired for neuropathic pain management. They found

maximal plasma concentrations of (R)-norketamine to reach 38.1 ng/ml and 34.9ng/ml (S)-norketamine within 23.3 minutes by a 20mg injection, 188.1 ng/ml and 172.0 ng/ml within 50 minutes via 50mg oral tablet, and 25.3 ng/ml and 21.3 ng/ml within 100-120 minutes via nasal spray. We expanded the drug concentrations on both the lower and higher ends of the spectrum of anticipated clinical blood plasma levels to ensure subclinical levels of Ketamine and Xylazine and levels beyond the point of expected anesthesia. A limitation to this, as mentioned in previous literature, is that in our ex-vivo model we are analyzing the effects of the drugs themselves and not any contributions of their active metabolites that are seen in blood plasma samples. For example it is well documented that norketamine plays an active role as it also possess anesthetic properties. If norketamine was administrated into the solution in addition to our Ketalar concentration it is possible we could have had additional effects on retinal ganglion cell function. This statement also holds true for Xylazine, as within an in-vivo model there is first-pass metabolism into multiple metabolites.

Xylazine plasma concentrations reported in the literature are variable among groups but there is a trend of lower concentrations compared to those found with ketamine. Garcia-Villar and colleagues (1981) investigated the pharmacokinetics of xylazine in larger mammals and found the peak plasma concentrations 15 minutes in sheep, dogs and horses was between 0.001 to 0.01mg/ml respectively. Latzel (2012) found the plasma concentrations of xylazine peaked between 0.0007 mg/ml to 0.003mg/ml in male/female mules and horses respectively.

When co-administered in both young and older Sprague-Dawley Rats ketamine plasma levels peaked around 0.01mg/ml in young rats 15 minutes after administration with a lower concentration found in older rats. Xylazine blood plasma concentrations peaked around 0.001mg/ml in young rats and showed a much lower concentration in older rats 15 minutes after administration (0.0003mg/ml) (Veilleux-Lemieux, 2013).

Plasma concentration is a useful and easy HPLC technique to quantify the pharmacokinetic of drug absorbed following different routes of administration. However, it does not necessarily reflect adequately the level of anesthetic

accumulation in tissues. For instance, it is recognized that anesthetic concentration in the brain can reach 5 times the level of the plasma one (Stoelting, 1999). Furthermore, anesthetic requirements for injectable anesthetics are much higher in small animals compared with humans, by a factor of 10 for ketamine and a factor of 100 for Propofol (Loepke & McGowan(2008). The range of anesthetic dissolution in the Ames' solution delivered to the MEA apparatus reflects these realities.

7.4 EFFECT OF ANESTHETIC AGENTS ON NEURONAL FUNCTION

General anesthetics such as ketamine and xylazine have been used for many years, however the related neurophysiological mechanism has yet to fully unfold. An extension of the central nervous system, the retina transmits visual information from the eye to the brain in trains of action potentials originating from retinal ganglion cells (Zeck, G., Lambacher, A. & Fromherz, P., 2011). A single visual stimulus excites dozens of different types of ganglion cells, each of which responding with a different latency to the same stimulus due to presynaptic circuitry shaped by specific types of interneurons. Using rabbit retina Zeck et al (2016) imaged the initiation and transmission of light-evoked action potentials along individual axons and found intraretinal condition increases the spike timing difference among ganglion cells of different types. Therefore the fastest ganglion cells act as indicators of a new stimulus for postsynaptic neurons.

Both anesthetics are known to have antagonistic effects on the central nervous system using various molecular mechanisms. Ketamine's main site of action appears to be within the thalamus and limbic systems, however suppression of respiratory drives are not seen until high doses are administered or small doses administered in high repetition (Stevenson, 2007).

Ketamine is known to have cortical effects on the brain at sub-anesthetic dosages. Musso et al (2011) had healthy participants perform visual tasks while simultaneously recording functional magnetic resonance imaging (fMRI) and electroencephalograms (EEG) while Ketamine/ Placebo was administered. Standard P300 amplitudes and latencies were determined for EEG data and found there was a

strong reduction in P300 amplitude in Ketamine conditions. Functional neuroimaging current density (CD) analysis showed a pattern of multiple current density maxima mainly located in the parietoocipital cortex with extension in the medial front brain region. The maxima were somewhat lower in the ketamine versus placebo condition with a significant current density maxima almost disappearing in the parietal cortex in the ketamine condition. Although the drug dependent P300 CD differences were relatively widespread, they were primarily seen in the areas of the parietrooccipital including visual association cortex. Interruption of NMDA mediated transmission (cortical micro-circuits) where paravalbumin-positive GABAergic interneurons are disinhibited by ketamine is a proposed mechanism by which ketamine effects connectivity changes within the brain circuitry (Joules et al, 2015;Homayoun & Moghaddam, 2007).

At low and intermediate drug concentrations we observed variable responses from RGC output but typically an increase in total spiking compared to baseline recordings. This becomes difficult to explain, however previous studies, although controversial, have proposed that NMDA antagonists may have neuroprotective features. In animal models of cerebral hypoxia/ischemia ketamine administration before and continued after insult shows a reduction in the neurodeficit (Kohrs & Durieux, 1998). When receptors are stimulated by very high levels of glutamate or aspartate the transmembrane flux and intracellular accumulation of Na and Ca leads to cell swelling and eventually death. Theories propose glutamate plays a key role in the neuronal injury signaling cascade and therefore suggests ketamine may be an appropriate therapy in some conditions such as cerebral ischemia/hypoxia. In particular rats treated with S(+) Ketamine have shown increased survival rate for damaged neurons and axonal growth, in relation to growth-associated protein GAP-43 (Kohrs & Durieux, 1998; Himmelseher et al, 1996).

At the highest concentrations both drugs showed a decline in the ratio of cell spiking compared to baseline spiking. Although controversial in the literature, one possible explanation to these findings are proposed by toxicity studies on human neurons, where ketamine was shown to induce toxicity via reactive oxygen species

(ROS)-involved mitochondria-mediated apoptosis pathway in a dose and time related fashion (Bosnjak et al, 2012). Typically ROS are formed as a natural byproduct of the metabolism of oxygen and play important roles in cell signaling. However during times of environmental stress ROS levels can increase resulting in signaling damage to cell structures. A more likely theory proposed is related to an osmotic shock model. The balance of hydration and solute concentration is key in maintaining equilibrium at the cellular level and plays a critical role on regulating normal functioning of a cell. Within an in-vivo model the osmolality is tightly controlled systemically by kidneys and blood supply. By removing the retinal tissue and performing experiments ex-vivo we have a disconnect from the body's normal kidney/blood regulation of hydration and solute concentrations (Finan & Guilak, 2010). Although the AMES solution helps simulate the in-vivo regulation of osmosis at our highest concentrations we could have created an osmotic shock where the anesthetics had a significant effect on ion-channel functioning, leaving the cell unable to respond or generate action potentials.

7.5 PROPOSED MECHANISM OF ACTION

Ketamine acts on the NMDA receptors in neurons in the central nervous system, but also interacts with the voltage-gated ion channels, including Ca2+ channels, delayed rectifier potassium channel, and hyperpolarization-activated cyclic nucleotide-gate channel, eventually leading to interference on synaptic transmission (Yuan, 2016). Yuan et al. found that Ketamine significantly inhibited the frequency and amplitude of spontaneous excitatory postsynaptic currents of pyramidal neurons in the primary somatosensory cortex of the Sprague-Dawley rats, however it failed to decrease the frequency of glutamatergic miniature excitatory postsynaptic currents. The amplitude of the glutamatergic miniature excitatory postsynaptic currents was decreased with Ketamine in a concentration-dependent manner. The authors used channel blockers to target the sodium current channels and found that the sodium current channels were predominantly involved in the ketamine-induced decreases in the frequency of the spontaneous excitatory

postsynaptic currents of cortical neurons. Additionally Ketamine decreases the amplitude of glutamatergic miniature excitatory postsynaptic currents without affecting the frequency indicating that ketamine acts post-synaptically to decrease the sensitivity of the glutamatergic receptors (Yuan, 2016). Another proposed molecular target of ketamine are HCN channel subunits that underlie a hyperpolarization-activated pacemaker current implicated in neuronal rhythmogenesis (Chen et al, 2009). Using a HCN1 knock-out mouse model, Chen et al (2009) concluded that ketamine caused HCN1-dependent membrane hyperpolarization and synaptic enhancement, which was strongly correlated to ketamine causing hypnosis. Anesthetic agents have also been studied on their proposed effect on certain 'leak' K+ channels in mammals, where increased K+ conductance leads to hyperpolarization, reduced responsiveness to excitatory synaptic input and altered network synchrony (Hemmings et al, 2005). Mice models of TREK-1 two pore domain K+ channel deletions showed a reduced sensitivity to immobilization by volatile anesthetics (Heurteaux et al 2004; Hemmings et al 2005).

Xylazine has been demonstrated to change the concentration of amino acid neurotransmitters such as glutamate and γ-aminobutyric-acid (GABA), which in both cases may induce nervous system disease (Yin et al, 2011). After the brain tissue from Sprague-Dawley rats were injected with xylazine, thalamencephal concentrations of GABA changed compared to controls. Within the hippocampus glutamate concentrations reached a minimum value at 0.25h after injection compared to control rats what showed a maximum value of glutamate concentration at this time (Yin et al, 2011). Thus, xylazine showed an inhibition of glutamate and facilitated GABA release mechanisms in rats.

Synaptic transmission plays a major role in the integration of neural activity within the central nervous system, while synapses have shown to be a major target of anesthetics. A synaptic transmission is triggered by the influx of Ca2+ to the presynaptic membrane and consequently neurotransmitters such as glutamate, GABA and acetylcholine are released (Yuan, 2016). Anesthetics affect synaptic transmission along multiple paths including presynaptic neurotransmitter release, postsynaptic neurotransmitter reuptake and the interactions of postsynaptic

receptors (Yuan, 2016). Voltage gated Na^+ channels, an essential piece to axonal conduction and synaptic integration/ neuronal excitability may also play a crucial role during anesthesia. The inhibition of presynaptic Na^2 channels in mammals has been correlated with the depression of evoked neurotransmitter release and synaptic transmission by volatile anesthetics such as isoflurane (Schlame & Hemmings, 1995; Hemmings et al, 2005).

Changes in synaptic transmissions may correlate with changes seen in cell tonicity and speed of responses. We observed when ketamine was administered to the retinal preparation at lower to intermediate dosages the RGCs responding to ON stimuli showed more sluggish responses (Figure 12) while OFF responses maintained a more consistent sustain response properties. The reverse effect was observed in the xylazine experiments; where with increased concentration of the drug the more prompt/brisk the responses were from RGCs responding to ON- and OFF- stimuli.

7.6 LIMITATIONS

There is much variability in recorded blood plasma concentrations of both drugs within the literature at various levels of anesthesia, amongst human and animal models. This variability can also be seen when attributed to age differences among the same species. When administrating xylazine among difference species Garcia-Villar et al. (1981) noted a small variation in drug distribution by intravenous route, however when administered intramuscularly the plasma concentrations were non-detectable in cattle. Within the same species of horse the difference to reach peak plasma concentration levels varied between intravenous and intramuscular routes. The degree of variability may account for the high levels of metabolism of the drugs, as very little unchanged xylazine is found in the urine collected (Garcia-Villar et al, 1981). In some species, such as cattle, there is a high sensitivity to the anesthetic where effects of deep sedation/analgesia are produced at lower dosages, however the plasma concentrations obtained may be 6-7x lower compared to other large animals such as horses (Hopkins, 1972). Even within a

human model there is variability of plasma concentrations of ketamine obtained between adult and pediatric/ infant subjections, which may be attributed to variable degrees of metabolic processes (Clements & Nimmo, 1981; Saarenmaa et al, 2001). The age difference was also noted in young Sprague-Dawley rats compared to older Sprague-Dawley rats where the half-life of xylazine went from 1.3 hours to 8.5-13 hours respectively (Veilleux-Lemieux et al, 2013). All anesthetic concentrations were calculated based on literature review on blood plasma levels of each drug found in rodents and other mammals at various levels of sedation. Plasma concentration alone may lack as an indicator of drug concentration effectiveness. Stoelting (1999) noted that plasma concentration began to decrease before the peak pharmacological effects of the drug manifested in subjects.

A possible limitation to the use of the MEA is insufficient contact between the tissue and electrodes, which may cause a poor signal to noise ratio; insufficient oxygenation/nutrient supply to ganglion cells; and possible movement of the retina during experimentation (Reinhard et al, 2014).

An additional limitation was that although robust and reproducible retinal ganglion cell recordings were obtained from retinal preparations the ERGs, which have been recorded by other authors, were not studied during these experiments. There are current investigations into ERG waveform morphology in the guinea pig retina, specifically as to where the b-wave is arising from and if this is truly similar to humans.

The ex-vivo model also creates a limitation in which the body's natural metabolic processes and secondary biological effects (i.e. cardiovascular effects) are not taken into consideration. The pharmacokinetics of ketamine have been studied in depth with known metabolites contributing to the anesthetic properties of the drug. Approximately 80% of Ketamine is metabolized to norketamine, which has been described as an active metabolite with one-third to one-fifth the activity compared to racemic ketamine (Mion & Villevieille, 2013; Potter & Choudhury, 2014). Xylazine pharmacokinetics are less known but do show many active metabolites that potentially play a role in its anesthetic properties. By isolating the retina in an ex-vivo model have removed any first pass metabolism, which occurs in

the body and hence had no active metabolites in our samples. The metabolic process has also shown to vary when both drugs are co-administered, where ketamine appears to reduce the clearance of xyalzine in the rat liver (St-Germain Lavoie et al, 2012; Veilleux-Lemieux et al, 2013). At the same time, this absence of systemic factors in the ex vivo preparation can be used to study the neuronal impact in isolation of confounding systemic factors. MEA studies are thus more oriented toward basic mechanistic comprehension of physiological phenomenon and less suitable to clinical interpretation.

7.7 FUTURE STUDIES

The pharmacokinetics of many anesthetics are well studied, however how these changes effect cell communication and output are still controversial and need further investigation. The guinea pig model has proven to be a suitable animal based model for human retinal disease, however there needs to be further investigations into these two anesthetics used during research. A plasma concentration calculation of both ketamine and xylazine should be conducted to confirm blood plasma concentrations of the active anesthetic and their metabolites during sedation. Additionally, our future study will include combining the two drugs at appropriate blood plasma concentrations to evaluate any potential additive effects the anesthetics would have on RGC spiking while both are present on the retinal preparation.

Additional investigations on the effects of ketamine when NMDA receptors of Nav1.1 isoforms are antagonized would help further document the mechanisms by which anesthetics exert their effects on neuronal plexuses.

Building upon the current data set one could look at the retinal interspike interval ISI, which may provide new insights on the ways spiking activity is influenced by anesthetics.

7.8 CONCLUSION

Retinal ganglion cell output is affected by anesthetics at clinical and above clinical dosages. The anesthetic properties appear to alter cell firing patterns and behaviors of the retinal ganglion cells within the ex-vivo model. Surprisingly, neuro tissue when isolated from metabolic processes is resistant to high concentrations of the anesthetics. At our lower dosages we see ketamine increasing the mean spiking ratio firing of those RGCs responding to ON and OFF stimuli but making the responses more sluggish when the dosage exceeded clinical blood plasma concentrations. In the opposite direction we observed more prompt responses at higher concentrations of xylazine on the RGCs responding to ON stimuli. General anesthetics have several mechanisms of action, which affect neural processing, which in turn has an effect on our visual system and visual processing. At clinical dosages patterns of RGC activity shift, which in theory alter the spike train signal to higher visual, processing centers. When using animal studies these factors need to be considered when investigating retinal, or cortical physiology.

REFERENCES

Ahmed, F., Hegazy, K., Chaudhary, P. & Sharma, S.C. (2001). Neuroprotective effect of α2 agonist (brimonidine) on adult rat retinal ganglion cells after increased intraocular pressure. *Brain Research*, 913, 133-139.

Arshavsky, VY., Lamb, TD. & Pugh, EN. (2002). G proteins and phototransduction. *Annual Review of Physiology, 64*, 153-87.

Arshavsky, V.Y. & Wensel, T.G. (2013). Timing is Everything: GTPase Regulation in Phototransduction. *Investigative Ophthalmology & Visual Science* Vol. 54, 7725-7733

Azeredo da Silveira, R. & Roska, B. (2011). Cell types, circuits, computation. *Neurobiology, 21*, 664-671.

Barry, M.J., Warland, D.K., & Meister, M. (1997). The structure and precision of retinal spike trains. *Neurobiology, 94*, 5411-5416.

Bear, M., Connors, BW. & Paradiso, MA. (2007). The Eye; Neuroscience: Exploring the Brain. Chapter 9 278-341. Lippincott Williams & Wilkins.

Bosnjak, Z., Yan, Y., Canfield, S., Muravyeva, M.Y., Kikuchi, C., Wells, C., Corbett, J. & Bai, X. (2012). Ketamine induces toxicity in human neurons differentiated from embryonic stem cells via mitochondrial apoptosis pathway. *Curr Drug Saf*. 7(2):106-119.

Brown, E.N., Purdon, P.L. & Van Dort, C.J. (2011). General Anesthesia and Altered States of Arousal: A systems Neuroscience Analysis. Annu Rev Neurosci; 34: 601-628.

Bui, B.V., & Fortune, B. (2003). Ganglion cell contribution to the rat full-field electroretinogram. *The Phyaiological Society*, *555*, 153-173.

Chen, X., Shu, S. & Bayliss, D.A. (2009). HCN1 Channel Subunits are a Molecular Substrate for Hypnotic Actions of Ketamine. *The Journal of Neuroscience*, 29(3): 600-609.

Choi, D.W. (1988). Glutamate neurotoxicity and diseases of the nervous system. *Neuron,* 1: 623-634.

Clements, J.A. & Nimmo, W.S. (1981). Pharmacokinetics and Analgesic effect of Ketamine in Man. Br. J. Anaesth 53:27-31.

Constantinescu, C.S. (2000). Constantin Von Economo's Theory of Primary Control of Sleep by the Central Nervous System. Proc R Col Physicians, Vol 30, 352-354

Craven, R. (2007). Ketamine. *Anaesthesia, 62*, 48-53.

Cringle, S., Yu, D., Alder, V., Su, E., & Yu, P. (1996). Oxygen consumption in the avascular guinea pig retina. *American Journal of Physiology, 271*,1162-1165.

Donello, J., Padillo, E., Webster, E., Dong, D., Madhu, C., Ling, J., WoldeMussie, E., Wheeler, L.A., Gil, D.W. (2000). Brimonidine inhibits the vitreal accumulation of glutamate and aspartate in the retinal transient ischemia model. Invest. Ophthalmol. Vis. Sci. 41 S831.

Finan, J.D. & Guilak, F. (2010). The effects of osmotic stress on the structure and function of the cell nucleus. J Cell Biochem; 109(3): 460-467.

Forman, S.A., & Chin, V.A. (2008). General anesthetics and molecular mechanisms of unconsciousness. *International Anesthesiology Clinics, 46 (3),* 43-53.

Franks, N.P. (2006). Molecular targets underlying general anesthesia. British Journal of Pharmacology, 147, S72-S81.

Garcia-Villar, R., Toutain, L., Alvinerie, M. & Ruckebusck, Y. (1981). The pharmacokinetics of xylazine hydrochloride: an interspecific study. *Journal of Vet. Pharmacol.* Therap. 4: 87-92.

Garfield, J.M., Garfield, F.B., Stone, J.C. et al (1972). A comparison of psychologic responses to ketamine and thiopental-nitrous oxide-halothane anesthesia. *Anesthesiology* 36:329-338.

Grasshoff, C., Drexler, B., Rudolph, U. & Antkowiak. B. (2006). Anaesthetic drugs: linking molecular actions to clinical effects. *Current Pharmaceutical Design, 12*, 3665-3679.

Greene, S.A., & Thurmon, J.C. (1988). Xylazine-a review of its pharmacology and use in veterinary medicine. *Journal of Veterinary Pharmacology and Therapeutics, 11*, 295-313.

Heavner, J.E. (2007). Local anesthetics. *Current Opinion in Anaesthesiology, 20,* 336-342.

Hemmings HC, Jr., Akabas MH, Goldstein PA, Trudell JR, Orser BA, Harrison NL. (2005). Emerging molecular mechanisms of general anesthetic action. *Trends Pharmacol* Sci.;26:503-10.

Heurteaux, C., Guy, N., Laigle, C., Blondeau, N., Duprat, F., Mazzuca, M., Lang-Lazdunski, L., Widmann, C., Zanzouri, M., Romey, G. and Lazdunksi, M. (2004). TREK-1, a K^+ channel involved in neuroprotection and general anesthesia. The EMBO Journal: 23, 2684-2695

Himmelseher, S., Auchter, M., Pfenninger, E., Georgieff, M. (1996). S(+)-ketamine prevents loss of mitochondrial transmembrane potential, increases glucose uptake and induces GAP-43 and MAP-2-expression in hippocampal neurons after glutamate exposure. *Anesthesiology*, 85:A711

Homayoun, H., Moghaddam, B. (2007). NMDA receptor hypofunction produces opposite effects on prefrontal cortex interneurons and pyramidal neurons. *Journal of Neuroscience* 43: 1196-11500.

Hopkins, T.J. (1972). The clinical pharmacology of xylazine in cattle. Australian veterinary Journal, 48: 109-112.

Idvall, J., Ahlgren, I., Aronsen, K.F., et al. (1979). Ketamine infusions: Pharmacokinetics and clinical effects. Br J ANaesth 51: 1167-1172.

Ikeda, Y., Oda, Y., Nakamura, T. Takahashi, R., Miyake, W., Hase, I. & Asada, A. (2010). Pharmacokinetics of Lidocaine, Bupivacaine, and Levoburpivacaine in Plasma and Brain in Awake Rats. *Anesthesiology*, 112: 1396-1403.

Jiulin, DU. & Xiongli, Y. (1999). Retinal bipolar cells- a model for the study of neuronal signal integration. *Chinese Science Bulletin, 44 No 19*, 1737-1743.

Joules, R. , Doyle, O.M., Schwarz, A.J., O'Daly, O.G., Brammer, M., Williams, S.C. & Mehta, M.A. (2015). Ketamine induces a robust whole-brain connectivity pattern that can be differentially modulated by drugs of different mechanism and clinical profile. *Psychopharmacology* 232: 4205:4218.

Juang, M.S., Konemura, K., Morioka, T. et al (1980). Ketamine acts on the peripheral sympathetic nervous system of guinea pigs. Anesth Analg (Cleve) 59:45-49.

Kalapesi, F.B., Coroneo, M.T., Hill, M.A. (2004). *Human ganglion cells express the alpha-2 adrenergic receptor: relevance to neuroprotection*. British Journal of Ophthalmology, 89, 758-763.

Kanda, T., & Hikasa, Y. (2008). Neurohormonal and metabolic effects of medetomindine compared with xylazine in healthy cats. *The Canadian Journal of Veterinary Research, 72,* 278-286.

Kefalov, VJ. (2011). Rod and cone visual pigments and phototransduction through pharmacological, genetic, and physiological approaches. *Journal of Biological Chemistry, 287,* 1635-1641

Kohrs, R. & Durieux, M.E. (1998). Ketamine: Teaching an Old Drug New Tricks. Anesth Analg 87:1186-93.

Kolb, H. (1991). The Neural Organization of the Human Retina. In J.R. Heckenlively & G.B. Arden, *Principles and Practice of clinical Electrophysiology of Vision*. St. Louis: Mosby-Year Book, Inc.

Kolb, H. (2004). How the retina works. *American Scientist*, *91*, 28-35

Kolb, H. (2006). Functional Organization of the Retina. In J.R. Heckenlively & G.B. Arden, *Principals and Practice of Clinical Electrophysiology of Vision 2nd Ed*. MIT press Cambridge, Massachusetts, London England.

Latzel, S. T. (2012). Subspecies studies: Pharmacokinetics and Pharmacodynamics of a Single Intravenous Dose of Xylazine in Adult Mules and Adult Haflinger Horses. *Journal of Equine Veterinary Science*, 32: 816-826.

Lei, B. (2003). The ERG of guinea pig (*Cavis porcellus*): comparison with I-type monkey and E-type rat. *Documenta Ophthalmologica, 106*, 243-249.

Lin, S.L., Shiu, W.C., Liu, P.C., Cheng, F.P., Lin, Y.C., & Wang, W.S. (2009). The effects of different anesthetic agents on short electroretinography protocol in dogs. *Journal of Veterinary Medical Science,* 71(6), 763-768.

Loepke AW, McGowan FX. 2008. CON: the toxic effects of anesthetics in the developing brain: the clinical perspective. Anesthesia and Analgesia, 106:1664-69

Malinovsky, JM. , Servin, F., Cozian, A., Lepage, JY., & Pinaud, L. (1996). Ketamine and norketamine plasma concentrations after i.v., nasal and rectal administration in children. *British Journal of Anaesthesia 77,* 203-207.

Manookin, M., Weick, M., Stafford, B. & Demb, J. (2010). NMDA Receptor Contributions to Visual Contrast Coding. *Neuon*, 67: 280-293.

Martiniuc, A.V., & Knoll, A. (2012). Interspike interval based filtering f directional selective retinal ganglion cells spike trains. *Computational and Intelligence and Neuroscience, 2012*, 1-17.

McIvor Road Veterinary Center. (1994). Effects of xylazine on humans: a review. *Austrialian Veterinary Journal, 71 (9),* 294-295.

Miller, R.D. (2010). Anesthesia 7th edition. Churchill Livingstone, Elsevier Inc.

Mion, G., & Villevieille, T. (2013). Ketamine pharmacology: an update (pharmacodynamics and molecular aspects, recent findings). *CNS Neuroscience & Therapeutics, 19,* 370-380.

Moreno-Bote, R. (2014). Poisson-Like Spiking Circuits with Probabilistic Synapses. PLoS Comput Biol 10(7): e1003522. doi:10.1371/journal.pcbi.1003522

Multi Channel Systems MCS GmbH. (2005). *Microelectrode Array (MEA) User Manual*. Reutlingen, Germany: Multi Channel Systems MCS GmbH.

Musso F., Brinkmeyer, J., Ecker, D. London, M.K., Thieme, G., Warbrick, T., Wittsack, H., Saleh, A., Greb, W., Boer, P. & Winterer, G. (2011). Ketamine effects on brain function-Simultaneous fMRI/EEG during visual oddball task. *NeuroImage 58, 508-525*

Nair, G., Kim, M., Nagaoka, T., Olson, D.E., Thule, P.M., Pardue, M.T. & Duong, T.Q. (2011). Effects of Common Anesthetics on Eye Movement and Electroretinogram. *Doc Ophthalmol,* 122(3), 163-176.

Niedorf, F., Bohr, H. & Kietzmann, M. (2003). Simultaneous determination of ketamine and xylazine in canine plasma by liquid chromatography with ultraviolet absorbance detection. Journal of Chromatography B 791: 421-246.

Nguyen-Ba-Charvet, KT & Chedotal, A. (2014). Development of retinal layers. *Comptes Rendus Biologies*, *337*,153-159.

Pai, A., & Heining, M. (2007). Ketamine. Continuing Education in Anaesthsia, Critical Care & Pain, 7, 59-63.

Peichl, L., & Gonzalez-Soriano, J. (1994). Morphological types of horizontal cell in rodent retinae: A comaprision of rat, mouse, gerbil, and guinea pig. *Visual Neuroscience,* 11, 501-517.

Pillow, J.W., Paninski, L., Uzzell, V.J., Simoncelli, E.P., & Chichilnisky, E.J. (2005). Prediction and decoding of retinal ganglion cell responses with probabilistic spiking model. *The Journal of Neuroscience, 25(47),* 11003-11013.

Potter, D.E., & Choudhury, M. (2014). Ketamine: repurposing and redefining a multifaceted drug. *Drug Discovery Today, 19,* 1848-1854.

Pluteanu, F., Ristoiu, V., Flonta, M.L. & Reid, G. (2002). A1-adrenoceptor-mediated depolarization and B-mediated hyperpolarization in cultured rat dorsal root ganglion neurons. Neuroscience Letters, 329, 277-280

Potyk, D.R., & Raudaskoski, P. (1998). Overview of anesthesia for primary care physicians. *West J Med, 168,* 517-521.

Povysheva, N.V. & Johnson, J.W. (2012). Tonic NMDA receptor-mediated current in prefrontal cortical pyramidal cells and fast-spiking *interneurons. Journal of Neurophysiology*, 107(8): 2232-2243.

Pugh, E.N. & Lamb, T.D. (2000). Phototransduction in vertebrate rods and cones: molecular mechanisms of amplification, recovery and light adaptation. In Stavenga, W.J. de Grip and E.N. Pugh, *Handbook of Biological Physics, 3* (Chapter 5, 183-255). Jr. Elsevier Science B.V.

Purves, D. Augustine, GJ., Fitzpatrick, D., et al. (2001). *Neuroscience 2nd edition. Glutamate Receptors*. Sunderland Associates. https://www.ncbi.nlm.nih.gov/books/NBK10802/

Pycock, C. (1985). Retinal neurotransmission. *Survey of Ophthalmology, 29*. 355-365

Racine, J., Joly, S., Rudiange, M., Rosolen, S. Casanova, C. & Lachapelle, P. (2005). The photopic ERG of the albino guinea pig (*Cavis porcellus*): A model of human photopic ERG. *Documenta Ophthalmologica 110*, 67-77.

Racine, J., Behn, D. & Lachapelle, P. (2008). Structural and functional maturation of the retina of the albino Hartley guinea pig. *Documenta Ophthalmologica, 117*, 13-26.

Rathbun, D.L., Alitto, H.J., Weyand, T.G., & Usery, W.M. (2007). Interspike interval analysis of reinal ganglion cell receptive fields. *Journal of Neurophysiology, 98*, 911-919.

Reinhard, K., Tikidji-Hamburyan, A., Seitter, H., Idrees, S., Mutter, M., Benkner, B., & Munch, T.A. (2014). Step-by-step instructions for etina recordings with perforated multi electrode arrays. *PloS ONE 9 (8): e106148. Doi:10.1371/journal.pone.0106148.*

Remington, L.A. (2005). The Retina. In *Clinical Anatomy of the Visual System (55-86)*. St. Louis: Elsevier, Inc.

Rudolph, U., & Antkowiak, B. (2004). Molecular and neuronal substrates for general anaesthetics. *Nature Reviews Neuroscience, 5,* 709-720.

Ryu, S.B., Ye, J.H., Lee, J.S., Goo, Y.S., Kim, C.H. & Kim, K.H. (2009). Electrically-evoked Neural activities of rd1 Mice Retinal Ganglion Cells by Repetitive Pulse Stimulation. Korean J Physiol Pharmacol, 13(6): 443-448.

Saarenmaa, E., Neuvonen, P.J., Huttunen, P. & Fellman, V. (2001). Ketamine for procedural pain relief in newborn infants. Arch Dis Child Fetal Neonatal Ed, 85: F53-F56.

Schlame, M. and Hemmings, H.C., Jr. (1995) Inhibition by volatile anesthetics of endogenous glutamate release from synaptosomes by a presynaptic mechanism. Anesthesiology 82, 1406–1416

Segev, R., Goodhouse, J., Puchalla, J., & Berry, M.J. (2004). Recording spikes from a large fraction of the ganglion cells in a retinal patch. *Natural Neuroscience, 7 (10),* 1155-1162.

Silva-Torres, L.S., Velez, C., Alvarez, L., & Zayas, B. (2014). Xylazine as a drug of abuse and its effects on the generation of reactive species and DNA damage on human umbilical vein endothelial cells. Pharmacology and Toxicology Department, School of Medicine, University of Puerto Rico, Medical Science Campus; San Juan, USA.

Son, Y. (2010). Molecular mechanisms of general anesthesia. *Korean Society of Anesthesiologists, 59(1),* 3-8

Spyridaki, M.H., Lyris, E., Georgoulakis, I., Kouretas, D. Konstantinidou, M., & Georgakopoulos, C.G. (2004). Determination of xylazine and its metabolites by GC-MS in equine urine for doping analysis. *Journal of Pharmaceutical and Biomedical Analysis, 35*, 107-116.

Stevenson, C. (2007). KETAMINE: A REVIEW Dr Carl Stevenson, Medecins Sans Frontieres Anaesthetist.

St-Germain Lavoie, D., Pailleux, F., Vachon, P. & Beaudry, F. (2012). Characterization of xylazin metabolism in rat liver microsomes using liquid chromatography-hybrid triple quadrupole-linear ion trap-mass spectrometry. *Biomedical Chromatography,* 27:882-888.

Stoelting, R.K. (1999). Pharmacology & Physiology in anesthetic practice. Philadelphia : Lippincott Williams & Wilkins. USA.

Stoelting RK. Pharmacology and physiology in anesthetic practice. Chapter 5 Bensodiazepines. Lippincott Williams & Wilkings, Philadelphia, third edition, 1999, pp148-151

Tremblay, F., & Parkinson, J.E. (2003). Alteration of electroretinographic recordings when performed under sedation or halogenate anesthesia in a pediatric population. *Documenta Ophthalmologica*, *107*, 271-270.

Tsukahara, Y., Blair, N.P., Spellman Eappen, D.C., Moy, J.J., Takahashi, A., Shah, G.K., Viana, M.A.G. (1992). *Ketamine Suppresses Ischemic Injury in the Rabbit Retina.* Investigative Ophthalmology & Vision Sciences, Vol. 33, No.5.

Urman, R.D. & Desai, S. (2012). History of anesthesia for ambulatory surgery. Lippincott Williams & Wilkins, 0952-7907 Walters Kluwer Health. (www.co-anesthesiology.com Vol 25, Number 6, December 2012).

Veilleux-Lemieux, D., Castel, A., Carrier, D., Beaudry, F., & Vachon, P. (2013). Pharmacokinetics of ketamine and xylazine in young and old Sprague-dawley rats. *Journal of American Association for Laboratory Animal Science, 52,* 567-570.

White, P.F., Way, W.L., Trevor, A.J. (1982). Ketamine-Its Pharmacology and Therapeutic Uses. *Anesthesiology* 56: 119-136.

WHO, Expert Committee on Drug Dependence, thirty-fourth report. Critical review of ketamine 2006.

Wilcock, A. & Twycross, R. (2011). Therapeutic reviews: Ketamine. *Journal of Pain and Symptom Management, 41*, 640-650.

Wood, L. (2010). Regulation of retinal activity in an ex-vivo guinea pig model by experimental conditions and effects of isoflurance and propofol anesthetics. Dalhousie University Master of Clinical Vision Science Program, 1-112.

Wood L, Windisch R, Parkinson J, Tremblay F. (2009). Animal models of human retinal activity: electroretinographic studies. Canadian Ophthalmological Society, Toronto.

Yanagihara, Y. et al. (2003). Plasma concentration profiles of ketamine and norketamine after administration of various ketamine preparations to healthy Japanese volunteers. *Biopharmaceutics & Drug Disposition, 24,* 37-43.

Yasuhara, K., Kobayashi, H., Shimamura, Y., Koujitani, T., Onodera, H., Takagi, H., Hirose, M., & Mitsumori, K. (2000). Toxicity and blood concentrations of xylazine and its metabolite, 2,6-dimethylaniline, in rats after single or continuous oral administrations. *The Journal of Toxicological Sciences, 25 (2), 105*-113.

Yin, B., Wang, H, Gong, D., Li, G. & Gao, L. (2011). Effects of xylazine on glutamate and GABA contents in the hippocampus and thalamencephal in the rat. *Bull Vet Inst Pulway* 55: 537-539.

Yu, D.-Y., & Cringle, S.J. (2001). Oxygen distribution and consumption within the retina in vascularized and avascular retinas and in animal models of retinal disease. *Progress in Retinal and Eye Research, 20*, 175-208.

Yuan, C., Zhang, Y., Zhang, Y., Cao, S., Wang, Y., Fu, B. & Yu, T. (2016). Effects of Ketamine on Neuronal Spontaneous Excitatory Postsynaptic Currents and Miniature Excitatory Postsynaptic Currents in the Somatosensory Cortex of Rats. *Iran J Med Sci, Vol 41 No 4,* 275-282.

Zeck, G.M., & Masland, R.H. (2007). Spike train signatures of retinal ganglion cell types. *European Journal of Neuroscience, 26,* 367-308.

Zeck, G., Lambacher, A., Fromherz, P. (2011). Axonal Transmission in the Retina Introduces a Small Dispersion of Relative Timing in the Ganglion Cell Population Response. PLoS ONE 6(6): e20810.doi:10.1371/journal.pone.0020810